AGU Books

Multi return periods flood hazards and risks assessment in the Congo River Basin

Journal:	*AGU Books*
Manuscript ID	2020-May-CH-1252.R1
Wiley - Manuscript type:	Chapter
Date Submitted by the Author:	n/a
Complete List of Authors:	Bola, Gode; University of Kinshasa Faculty of Sciences, Natural Resources Management; commissariat general a l'energie atomiqu Tshimanga, Raphael; na, Congo Basin Water Resources Research Center Neal, Jefferey; University of Bristol Hawker, Laurence; University of Bristol Muamba, Lukanda vincent ; University of Kinshasa Faculty of Sciences Trigg, Mark; University of Leeds, Civil Engineering Bates, Paul; University of Bristol, School of Geographical Sciences
Primary Index Term:	1719 - Hydrology < 1700 - HISTORY OF GEOPHYSICS
Index Term 1:	1821 - Floods < 1800 - HYDROLOGY
Index Term 2:	456 - Life in extreme environments < 400 - BIOGEOSCIENCES
Index Term 3:	468 - Natural hazards < 400 - BIOGEOSCIENCES
Index Term 4:	1817 - Extreme events < 1800 - HYDROLOGY
Keywords:	flood hazard, flood risk, return period, population exposure, Regional scale, Congo River Basin
Abstract:	Flood disasters have regularly been reported in the Congo Basin with significant damages to human lives, food production systems and infrastructure. Losses incurred by these damages are huge and represent a major challenge for economic expansion in developing nations. In the Congo River Basin, where availability of in-situ data is a significant challenge, new approaches are needed to investigate flood risks and enable effective management strategies. This study uses recently developed global flood prediction data in order to produce flood risk maps for the Congo River Basin, where flood information currently does not exist. Flood hazard maps that estimate fluvial flooding at a grid cell resolution of 3 arc-seconds (~ 90 m), gridded population density data of 1 arc-second (~ 30 m) spatial resolution, and a spatial layer of infrastructure dataset are used to addresses flood risk at the scale of the Congo Basin. The global flood data provides different return periods of exposure to flooding in the Congo Basin and identifies flood extents. The risk analysis results are presented in terms of the percentage of population and infrastructure at flood risk for six return periods (5, 10, 20, 50, 75 and 100 year). Of the 525 administrative territories, 374 are

	exposed to fluvial flood, and 38 (10 %) of them are categorised as risk hotspot. Analysis shows that the most exposed territories represent 1% of total exposure which is estimated at 2.65% of the basin's population. This study demonstrates the first and potentially most important stage in developing flood responses by determining the flood hazards areas and the population that would be exposed. The flood risk maps produced in this study provide information necessary to support policy decision of flood disasters prevention, including prioritisation of interventions to reduce flood risk in the CRB.

Multi return periods flood hazards and risks assessment in the Congo River Basin

Gode Bola[1], Raphael M. Tshimanga[1], Jeff Neal[2], Laurence Hawker[2], Mark A. Trigg[3], Lukanda Mwamba[4] , Paul Bates[2]

[1] *Congo Basin Water Resources Research Center (CRREBaC) & Department of Natural Resources Management, University of Kinshasa, DR Congo*

[2]*School of Geographical Sciences, University of Bristol, United Kingdom*

[3]*School of Civil Engineering, University of Leeds, United Kingdom*

[4]*General Commission of Atomic Energy, Regional Center for Nuclear Study, Kinshasa, DR Congo*

Abstract

Flood disasters have regularly been reported in the Congo Basin with significant damages to human lives, food production systems and infrastructure. Losses incurred by these damages are huge and represent a major challenge for economic expansion in developing nations. In the Congo River Basin, where availability of in-situ data is a significant challenge, new approaches are needed to investigate flood risks and enable effective management strategies. This study uses recently developed global flood prediction data in order to produce flood risk maps for the Congo River Basin, where flood information currently does not exist. Flood hazard maps that estimate fluvial flooding at a grid cell resolution of 3 arc-seconds (~ 90 m), gridded population density data of 1 arc-second (~ 30 m) spatial resolution, and a spatial layer of infrastructure dataset are used to addresses flood risk at the scale of the Congo Basin. The global flood data provides different return periods of exposure to flooding in the Congo Basin and identifies flood extents. The risk analysis results are presented in terms of the percentage of population and infrastructure at flood risk for six return periods (5, 10, 20, 50, 75 and 100 year). Of the 525 administrative territories, 374 are exposed to fluvial flood, and 38 (10 %) of them are categorised as risk hotspot. Analysis shows that the most exposed territories represent 1% of total exposure which is estimated at 2.65% of the basin's population. This study demonstrates the first and potentially most important stage in developing flood responses by determining the flood hazards areas and the population that would be exposed. The flood risk maps produced in this study provide information necessary to support policy decision of flood disasters prevention, including prioritisation of interventions to reduce flood risk in the CRB.

Keywords: Flood hazard, Risk assessment, Return period, Congo River Basin

1. Introduction

Floods are the most common and devastating natural disasters around the world (UNISDR, 2011; Ward et al., 2013; Tanoue et al., 2016). Globally, damages due to floods during the last four decades costed more than 1 trillion $ US, with a loss of about 220,000 human lives (Jonkman, 2005; Munich Re, 2019). For the year 2019 alone, at least 396 natural disasters were reported, killing 11755 people of which floods and storms accounted for 68% of the total number of affected people (EM-DAT, Guha-Sapir et al. www.emdat.be, 2019). Worldwide, about 1 billion people are living in areas at risk of flooding (Collet et al., 2018). Recent studies indicate an increase in flood exposure -people and assets- (Tanoue et al., 2016; Change et al., 2001; Ward et al., 2013; Visser et al., 2014), therefore highlighting the role of land use change (Milly et al.,2002 ; Bronstert, 2003; Christensen and Christensen, 2003) and climate change (Kundzewicz et al., 2014) in the increase of frequency and intensity of floods. In 2005 the World Bank Hotspots Project estimated risks based on reported flood event data combined with gridded population and GDP information (Dilley & Mundial, 2005). The United Nations International Strategy for Disaster Reduction (UNISDR) produced maps of population and GDP exposed to flooding using a combination of modelled and reported events (Peduzzi et al., 2009). Jongman et al. (2012) contributed further by quantifying changes in population and assets exposed to 100-year flood events between 1970 and 2050. Hirabayashi et al. (2013) quantified the impacts of future climate change on the number of people exposed to 10 and 100-year flood events. Ward et al. (2013) produced a global-scale flood risk maps based on a large number of return-periods with a module to simulate multiple risk indicators.

Floods are difficult to predict, this is basically due to limited understanding of processes governing the occurrence of flood hazards, which is exacerbated by limited access to data at the appropriate spatial and temporal scales. However, recent advances in computing power and better access to Earth Observation information have provided an unprecedented opportunity to better predict the occurrence of flood events and, thus reducing risks. Through this opportunity, models have been developed that produce flood extent outputs that are now freely available and being used to address science and management questions related to flood hazards and risks, including the issue of how flood risks could change in the future. For instance, Neal et al. (2012a) developed a subgrid channel model for simulating floodplain inundation over large and data sparse areas, based on combination of earth observation data, including water surface elevation from Ice, Cloud and Land Elevation Satellite laser altimeter. Schumann et al. (2013) developed a large-scale flood inundation model that uses ensemble forecasting data for flood prediction in data scarce areas, while Sampson et al. (2015) produced a 3 arc-second resolution global flood hazard maps for several return periods using

LISFLOOD-FP with regionalised flood frequency analysis derived from global hydrological data. Other global models based on processed versions of the SRTM DEM and HydroSHEDS river network such as CaMa-Flood (Yamazaki et al.,2011) and GLOFRIS (Ward et al., 2013) have been used to understand the implication of flood on exposed gross domestic product loss and population, both under current and future conditions of land use and climate change (Trigg et al., 2016; Winsemius et al., 2015).

Until recent years, the majority of studies have focused on global coverage. To date, national or regional flood hazard and risk studies have been undertaken mostly in developed countries, allowing a consistent and comprehensive understanding of their flood hazard and risk for planning. Some of these studies include (Roo et al., 2000; Fortin Jean-Pierre et al., 2001; Eleutério et al., 2010; Samarasinghe et al., 2010 ; Safaripour et al., 2012; Lim & Lee, 2018). In developing countries where the effects of floods are more pronounced due to low level of flood protection, there are far fewer works on flood hazards and risks due to the challenges of accessing appropriate data and the remoteness of some flood prone regions (Alcántara-Ayala, 2002; Baldassarre et al., 2010; UNISDR, 2015; Trigg et al., 2016 ; Egbinola et al., 2017). Recent advances in remote sensing technology, data processing algorithms and new satellite platforms have converted data poor regions of developing countries to data rich regions (Bates, 2012). Through modelling coupled with global data, flood hazards have been predicted and, when combined with vulnerability data, flood risk areas have been mapped out (Samarasinghe et al. 2010). In their study of watershed modelling and flood prediction, Samarasinghea et al. (2010) used a hybrid GIS and remote sensing-based approach for flood risk determination in Sri Lanka. By coupling remote sensing data with a multi-criteria decision analysis algorithm, an approach for flood risk assessment for the Kopili River Basin in India and Vietnam has been developed (Shivaprasad et al., 2018, Armenakis et al., 2017). Optical and radar remote sensing data along with logistic regression were used to develop modelling for flood-damaged areas in North Korea (Lim & Lee, 2018). Safaripour et al. (2012) perform flood risk assessment using Landsat imaging and a digital elevation model to assess flood risk in the Gorganroud watershed in Iran. These studies demonstrate that earth observation data coupled with Geographical Information Systems have proved resourceful for flood management in developing countries (Schumann et al., 2009; Mason et al., 2011). However, Sub-Saharan African countries have not taken enough the advantage of remote sensing or recent flood prediction and management data that assess flood hazard and risk. For instance, studies at regional scales, such as the Congo River Basin (CRB), where a large proportion of the population are at risk of flooding, have not yet been undertaken. Flood disasters have been regularly reported in the CRB with

significant damages to socio-economic well-being and to the environment. A diagnostic study on flood risk by Tshimanga at al. (2016) showed that from 1964 to 2012, the CRB has recorded about 196 flood events that have affected about 10 million people. Moreover, the impact of floods in forthcoming decades could increase in the CRB due to the current trend of land use changes as well as climate change (Ward et al., 2013, Kundzewicz et al., 2014). Therefore, there is a demand from end users (e.g. local institutions) for flood hazard and risk information, for example in terms of maps of flood-prone areas, assets, and population exposed. Increasing availability and constant improvement of high resolution (3 arc-seconds or ~ 90 m) earth observation data and their application in the data scarce basin of the CRB can help derive flood hazard and flood risk maps to meet end users' needs (Bates, 2012).

This study, therefore, uses the global flood data simulated using a global flood model based on LISFLOOD-FP (Sampson et al., 2015), in combination with socio-economic and population information to evaluate flood risks at the Congo Basin, With the aim to assist policy decision for flood mitigation, necessary to enhance communities' resilience in the Congo River Basin.

2. Study Area

The Congo River Basin (CRB) is framed within 10^{o} N, 12^{o} E to 14^{o} S, 34^{o} E (corner-corner coordinates, Fig. 1), and encompasses nine riparian countries. The central part of the basin has low slopes, but many of the headwaters have steeper topography, from which flow the four main Congo tributaries (the Oubangui River in the North East, Sangha River in the North West, the Kasai River in the South West, and the Lualaba River in the South East). These tributaries meet in the central basin and form the main stem of the Congo River (Tshimanga & Hughes, 2014). Many cities in the CRB are located near the major rivers and tributaries, such that fluvial floods constitute a major issue. It is estimated that 39 million people live within 10 km of a major river in the CRB (Trigg et al., 2020). A study by Tshimanga et al. (2016) determined that floods in the CRB occur in form of riverine floods, flash floods and other combined types of flood, such that riverine floods are the most prominent type of flood with 121 events recorded since 1964 in the region. As a natural hazard, floods often occur when the river system carrying capacity is unable to convey the river flow, especially after heavy rain has occurred in the basin. This situation can worsen when the flood prone areas have been developed for human use with little or no flood protection measures. Characterised by a tropical climate and with a high drainage density, the CRB is a classic example of a vast flood-prone region in Africa (Dilley et al., 2005).

The general pattern of CRB precipitation (Fig. 2) consists of two rainy seasons: March to May (MAM) and October to December (OND), which has higher rain rates (Pokam et al., 2014). The

driest season is from June to August (JJA). Flood occurrences coincide with rainfall peaks in the Congo Basin (Fig. 2), which often occur around November and December (Haensler et al. 2013). The CRB is identified as an important flooding hotspot (Dilley, 2005, Kundzewicz et al., 2014). For instance, the 2015 flooding affected 8,480 families in the CRB (Angola, Tanzania, Cameroon, and DRC) and resulted in 100 fatalities and 10,000 individuals displaced (Tshimanga et al., 2016). Furthermore, the recent 2019-2020 floods affected about 170,000 people across the Republic of the Congo, including 30,000 in Central African and Congolese refugees and 6,302 hectares of agricultural fields have been destroyed (Reliefweb, 2019). Floods have also been reported in many other parts of Democratic Republic of the Congo (DRC), notably in the provinces of Bas Congo and Kisangani (Tshimanga et al., 2016). In 1999, a flood occurred in November and lasted until January of the following year, thus approaching the two previous largest flood events of the century, in 1903 and 1962. The 1999 flood affected tens of thousands of people in both Kinshasa (DRC) and Brazaville (Republic of Congo) and caused serious disruption of the drinking water supply (Tshimanga et al., 2016).

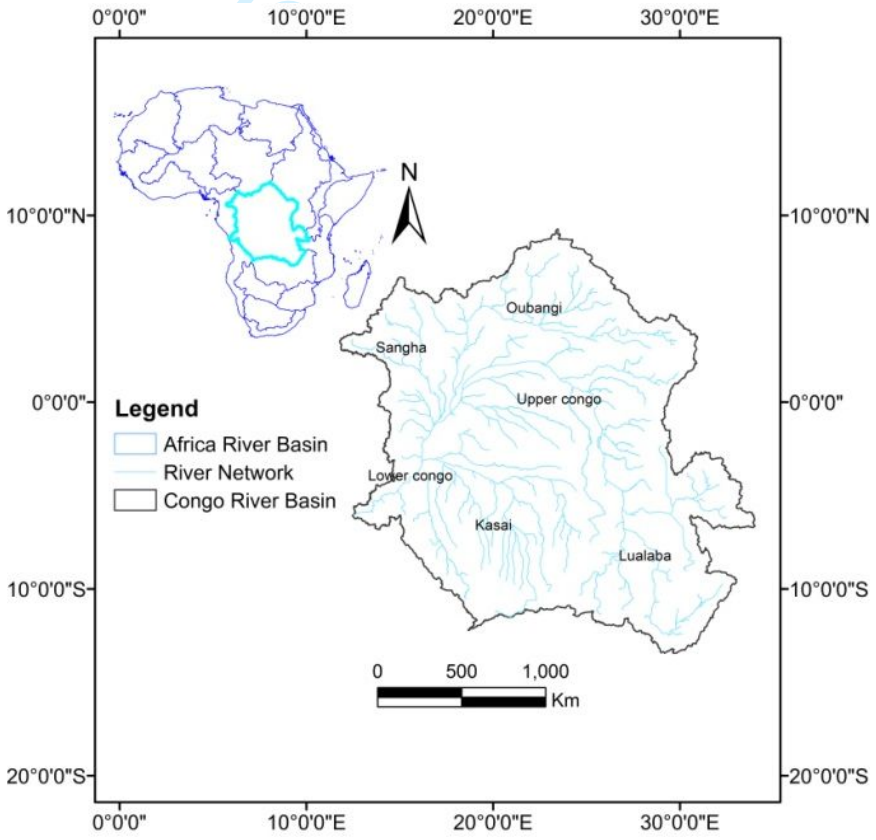

Figure 1: Congo River Basin

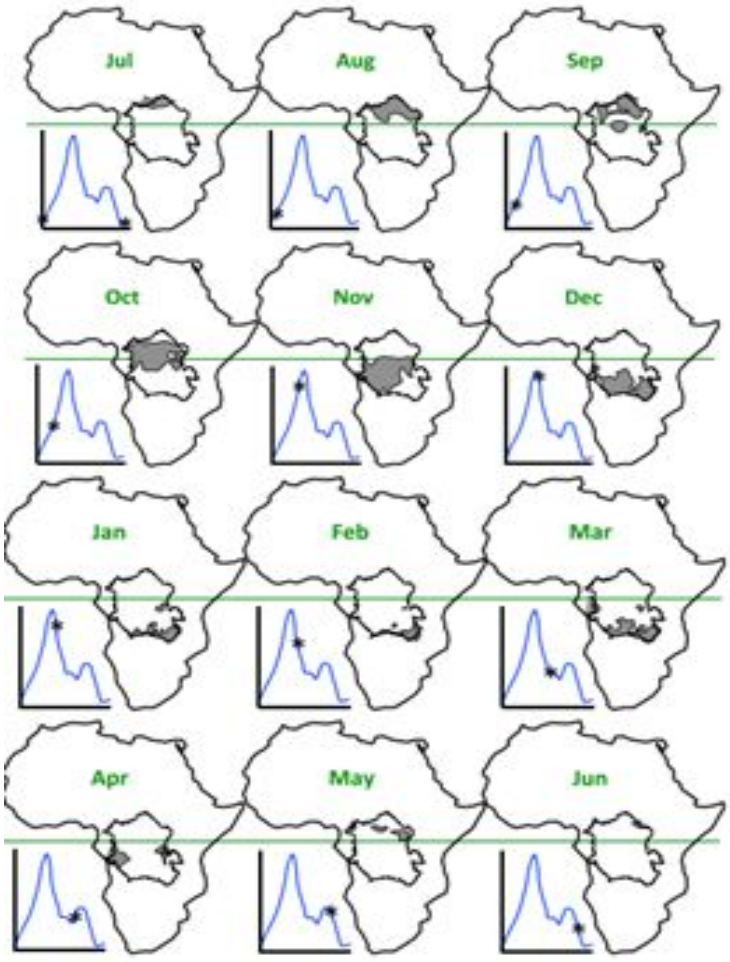

Figure 2: Rainfall and Congo River flow pattern. Grey indicates location for mean rainfall (JAS = 73mm month^{-1}, OND = 160 mm month^{-1}, JFM = 123 mm month^{-1}, AMJ = 146 mm month^{-1}). The hydrograph represents a July-June water year with long term average of Congo River discharge at Kinshasa gauging station. Asterisks mark the given discharge on the month (Jul = 29,991m^{3}s^{-1}, Aug = 29,035m^{3}s^{-1},Sep = 32,017 m^{3}s^{-1},Oct = 41,525 m^{3}s^{-1},Nov = 49,143m^{3}s^{-1}, Dec = 53,680 m^{3}s^{-1}, Jan = 45,505 m^{3}s^{-1}, Feb = 36,108 m^{3}s^{-1}, Mar = 33,559 m^{3}s^{-1}, April = 38,084 m^{3}s^{-1}, May = 40,883 m^{3}s^{-1}, Jun = 37,466 m^{3}s^{-1}), the green line marks the equator, (adapted from Alsdorf et al., 2016).

3. Flood Risk Analytical Framework

This research focuses on flood hazard, vulnerability and risk, and we adopt the definitions of these concepts are from UNISDR (2015). Flood hazard denotes the likelihood of a potentially damaging physical event that may cause the loss of life or injury, property damage, social and economic disruption, or environmental degradation that it is usually presented as an annual exceedance probability and/or return period.

Flood vulnerability encompasses a set of conditions and processes resulting from physical, social, economic, and environmental factors that increase the susceptibility of a community to the impact

of hazards (Merz et al. 2015). Exposure can be defined as the assets and values located in flood-prone areas (IPCC, 2012). Flood risk refers to the probability of harmful consequences, or expected losses (deaths, injuries, property, livelihoods, economic activity disrupted, or environment damaged) resulting from interactions between flood hazards and vulnerable conditions (UNISDR, 2015). Risk analysis can be realised at different scales (macro, meso and micro), depending on the objectives of the analysis. Different scales of risk evaluation are defined as a function of the level of detail of the evaluation process (Eleutério, 2012, de Moel et al., 2009, Schumann, 2011) of which in the CRB:

- Macro-scale refers to full spatial region of the Congo Basin;
- Meso-scale to the Congo Basin's sub-watershed level, such as the Oubangui for instance;
- Micro-scale is adopted if a single element such as administrative territory is analysed.

Different combinations of scales can be considered depending on the data availability, e.g. hazard maps produced using macro-scale methods can be combined with micro-scale exposure and vulnerability datasets in order to evaluate potential flood risk (de Moel, 2009). In developed countries, we can observe different scales of evaluation and a mixture of scales used in the literature (Messner & Meyer, 2006; Barredo et al., 2005; Eleutério, 2012). While macro and meso-scale flood analysis for developing countries can rely on global data, the proposed framework (Fig. 3) is applied at the regional scale (macro-scale) as micro-scale flood risk analysis requires financial and human resources as well as high resolution data, particularly for the data sparse regions such as the CRB.

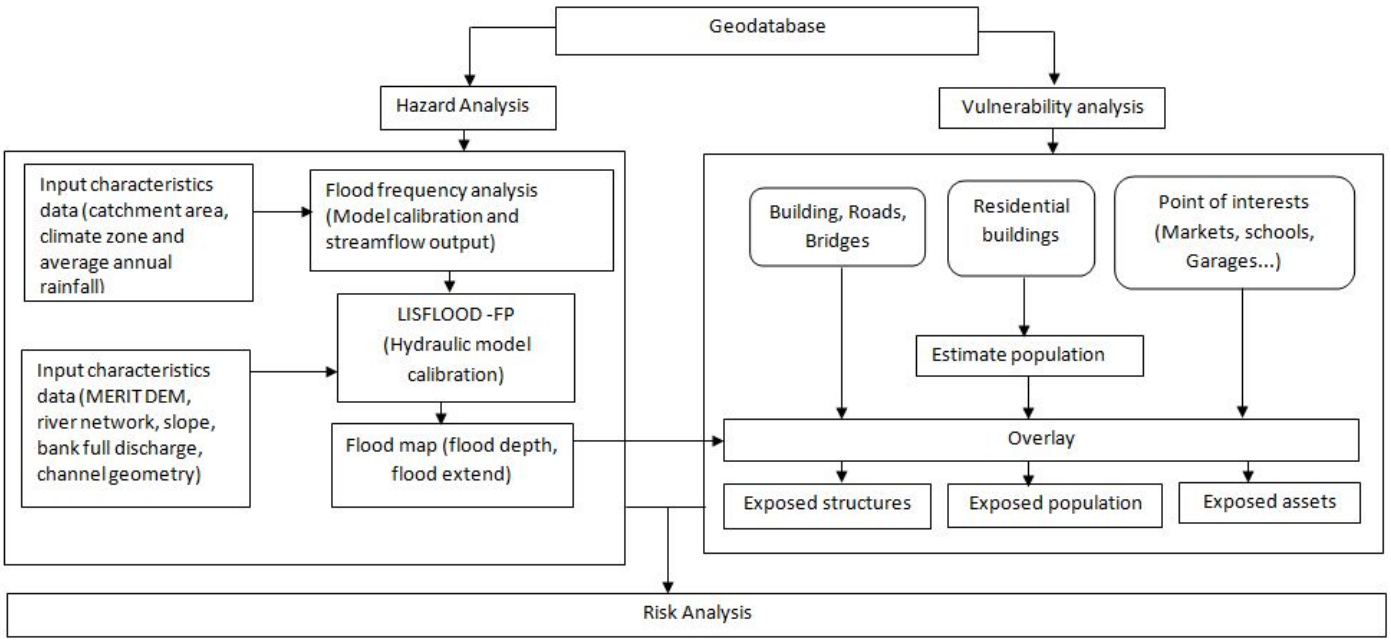

Figure 3: Flood risk analysis framework (modified from Bizimana and Schilling, 2010).

Such a regional scale assessment aims at the identification of risk areas in order to alert the public and inform policy decision makers of the potential risks. The identification of risk areas across nations is fundamentally concerned with controlling development in such areas and also for investment prioritisation (de Model et al., 2015).

4. Data and methods

To examine flood risk, we employ spatial data defining flood hazard and a number of socio-economic characteristics (infrastructure and buildings) and population density.

4.1. Flood Hazard Data

We used flood hazard maps (Sampson et al., 2015) produced using a variant of the LISFLOOD-FP hydrodynamic model representing riverine flood hazards for the CRB. The LISFLOOD-FP flood hazard maps estimate the inundation caused by fluvial flooding at a grid cell resolution of 3 arc-seconds (~ 90 m), for different return periods. The maps provide information on the extent of flood hazard for specific locations (Fig. 4). The flood hazard spatial layer consists of areas that are susceptible to flooding, such as water bodies, areas of low slope, floodplains and topographic depressions. For this study, six hazard return periods (5, 10, 20, 50, 75 and 100 year) were used. Modelled flood hazards do not include any flood protection (such as levees and drainage systems). However, flood protection is not yet implemented in many developing countries, particularly in the CRB.

Fluvial flooding is simulated in all river basins with upstream catchment areas larger than 50 km^2 (Smith et al., 2019). River channel locations are derived from the MERIT Hydro global hydrography data set (Yamazaki et al. 2019). A sub-grid hydraulic model (Neal, Bates, and Schumann 2012b) is used, which enables all river channels, even those smaller than the 3-arc second (~90 m) resolution of the model, to be explicitly represented using a computationally efficient local inertial formulation of the shallow water equations (Bates, Horritt, and Fewtrell 2010). Integration of a hydrography global data set with a sub-grid hydraulic model enables the representation of flooding from river channels across all areas, including data-poor regions (Sampson et al., 2015). The derived model input boundary conditions are from a global regionalised flood frequency analysis (Smith, Sampson, and Bates 2015). This method links river gauges to catchment characteristics and local climatology respectively, with un-gauged regions linked to gauged. Sampson et al. (2015) in their attempt to describe the areas affected by all flood events of a certain magnitude, report that the global model fairly captures between two thirds and three quarters of flooded area in the local benchmark data sets from Canada and the UK, and that along nontidal reaches of large rivers, the skill is likely close to that of local models. The model has been demonstrated to perform well for inland flooding, and MERIT DEM is used to enable the

model to simulate flood hazard on vegetated and urbanized floodplains. However, the model is likely to underestimate flood hazard in coastal areas that are prone to tidal flooding due to the lack of a storm surge component (Sampson et al., 2015). The model may also overestimate hazard along rivers with significant reservoir management capacity as such features are not yet incorporated (Sampson et al., 2015). As such, the LISFLOOD- FP output is suitable for flood analysis and management in the CRB. Users should not expect perfection from the model, but it is useful for describing areas exposed to a certain magnitude of flood and undertaking related flood risk analysis at the scale of interest (national and regional) which can be incorporated into decision making (Ward et al., 2015).

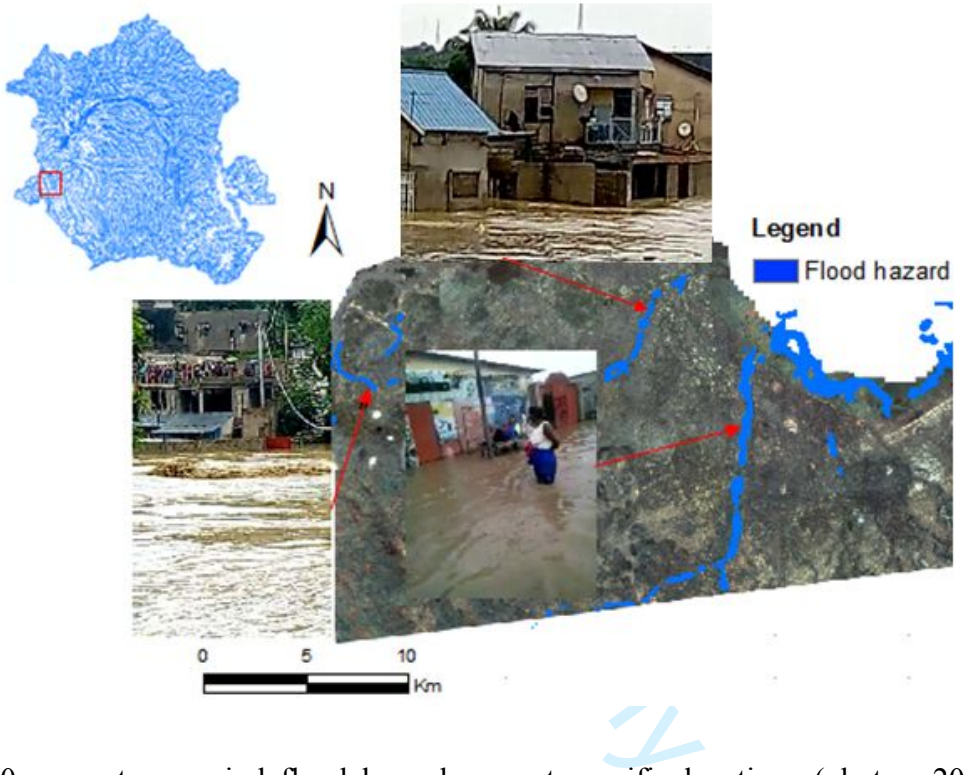

Figure 4: 100-year-return period flood hazard map at specific locations (photos, 2019 flood in Kinshasa)

4.2. Socioeconomic Data

To estimate the number of people exposed to flooding, we used a gridded population density data of 1 arc-second, (~ 30 m) spatial resolution. The CRB High Resolution Population Density Map is a new population dataset generated jointly by Facebook, Columbia University and the World Bank. Previous population maps (Bright et al., 2015, Tatem & WorldPop, 2017) represented population pixel with a spatial resolution of 3 arc seconds (LandScan), or ~100 m spatial resolution (WorldPop), but Facebook and Columbia University (2018) have achieved the spatial refinement (1 arc-second) based on a convolutional neural network to identify individual buildings. Based on the settlement identification, population is then redistributed equally over all the buildings found within

the census area. The method assumes equal population distribution per building within a census area. By combining the building data with census data, the population data with 1 arc-second (~ 30 m) spatial resolution was produced. The Third Integrated Household Survey (IHS3) which provides a descriptive analysis of the demographic characteristics of the population of Malawi (NSO, 2016) which has been completely manually labelled, at a resolution of 3 arcsecond was used to validate the data. Tiecke et al. (2017) outline a number of validation exercises for the High Resolution Population Density Map data, including the testing of building identification. This survey recorded the location of 12,288 households countrywide. When used as a validation data set, the results revealed that 95.3% of IHS3 household locations coincided with High Resolution Population cells/pixels. After assessing the accuracy of the buildings, the population redistribution over the buildings was undertaken for a single region of Blantyre, Malawi. Population estimates are obtained using a minimally modelled approach of proportional allocation (De Sherbinin & Adamo, 2015). The population is distributed equally to settled areas in the binary classification that fall inside census units. The uncertainty of the population estimates originates from census data obtained at a too coarse administrative unit. The full methodology of gridded population data can be found in Tiecke et al.(2017). Flood is also the result of the interactions of natural and human factors, this interplay is illustrated in Fig.5 and 6.

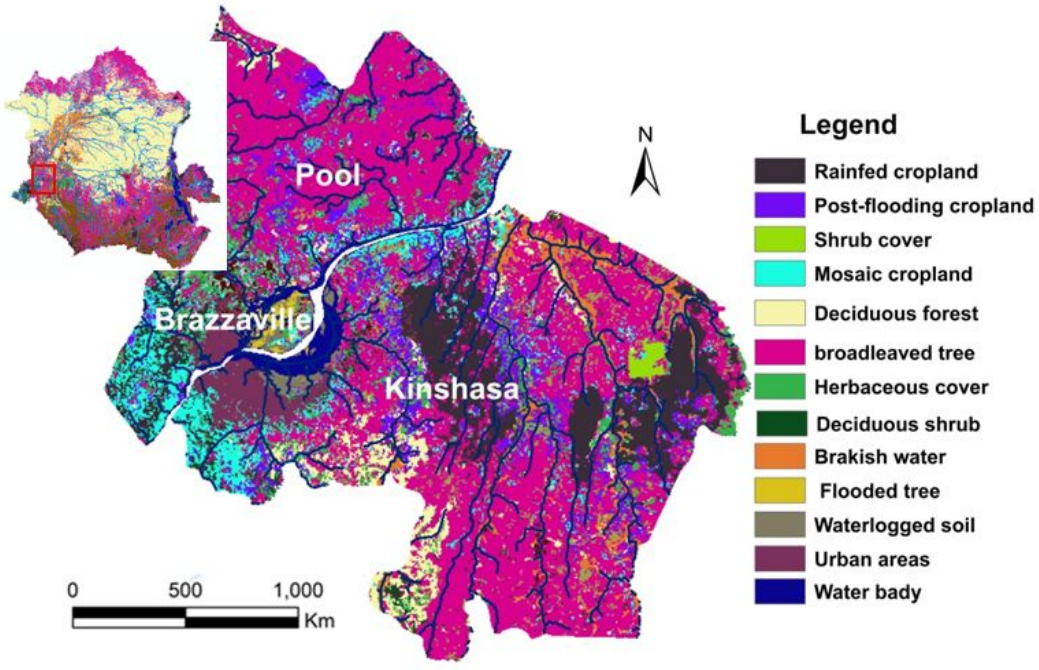

Figure 5: Land covers types illustrated by Kinshasa and Brazzaville

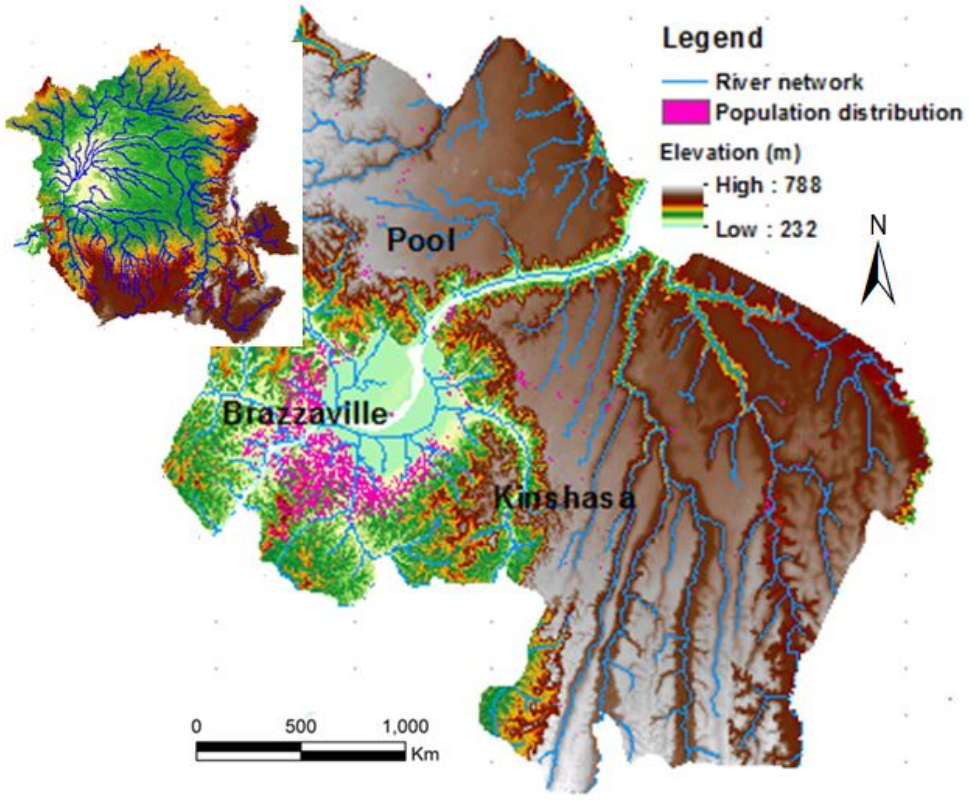

Figure 6: River network, terrain and population pixels distribution illustrated by Kinshasa and Brazzaville.

Spatial layers (Fig. 7) that contain the administrative areas (Map library, 2019) and population distribution have been used as units of investigation for this work. The total population and infrastructures in the Congo Basin was extracted from population pixel and infrastructures layer mentioned in the section above, and presented in table 1.

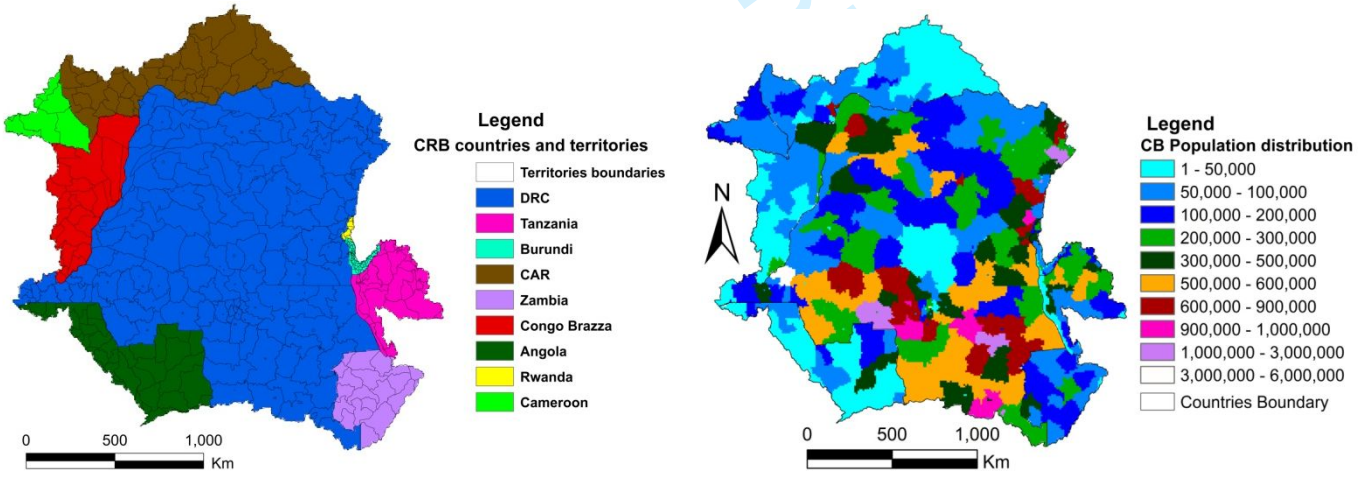

Figure 7: Congo Basin countries with 525 second level administrative subdivision (territory) and population distribution extracted from high resolution population pixels.

Table 1: Population and infrastructures within the basin

Countries	Elements	
	Population(millions)	Infrastructures
Democratic Republic of the Congo	73.60	5725
Zambia	3.28	101
Tanzania	6.39	149
Burundi	5.03	378
Rwanda	1.85	146
Central African Republic	3.55	237
Angola	2.35	9
Republic of Congo	3.02	428
Cameroon	0.86	261
Total	**99.93**	**7434**

The Humanitarian Openstreet MapTeam's spatial layers (HDX/OCHA, 2019) that contain urban system such as buildings, fuel stations, school, marketplaces, and hotels have also been used.

Community of mappers all over the world work together online, using satellite, GIS software and drone imagery to generate map layers of infrastructure including buildings, roads, shops, businesses, rivers, topographical peaks, administrative boundaries, bus and train routes in OpenStreetMap. The resulting free map layers are made available online via the Humanitarian Data Exchange (HDX) and can be used for disaster management and risks reduction. In case of the Congo River Basin, these maps (Fig. 8) represent the spatial distribution of infrastructure and buildings and helped us to map and understand risk related to flooding. OpenStreetMap data cover all CRB, but is far from complete because all objects are not mapped. Therefore, infrastructure numbers are only indicative of exposure in the CRB.

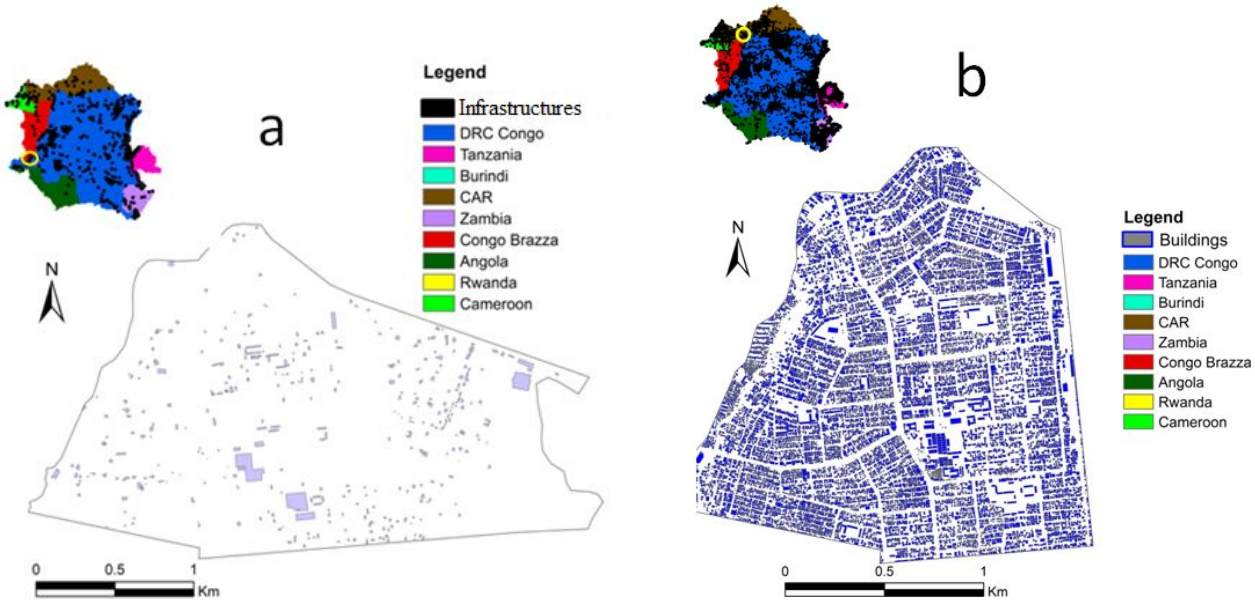

Figure 8: Town level maps, showing spatial representation of infrastructures and buildings in two urban areas: (a) infrastructures distribution in Kinshasa; (b) buildings distribution in Bangui (Source: Humanitarian OpenStreetMap spatial layers).

4.3. Methods

4.3.1. Flood exposure

The analysis in this study was done in QGIS (v3.10). The population gridded dataset (1 arc-second resolution) were resampled to the same resolution (~90 m) as the flood dataset (3 arc-second resolution) using the nearest neighbour method. The number of people or infrastructure (road and bridges, healthcare facilities, educational institutions, police, buildings and fuel stations) exposed to each return period were estimated per territory. The raster calculation method was used to produce the flood exposure layer, intersecting flood hazards pixels with the spatially distributed population gridded data, to extract people per population grid cell within flood hazards pixels which represent the flood exposed population pixels. Flood exposure at territory level for each return period flood hazard was estimated by calculating the sum of population pixels of flood exposure layer overlaying territory polygons through zonal statistics. We run this analysis for all the return periods at a territory level and aggregate our results at country and basin level to estimate the total number of people affected. Therefore, flood risk for the population (R_f), was defined by the equation (1).

$$R_f = F_h \cap S_p \quad (1)$$

Were,

R_f: is flood risk for each territory

F_h: is the flood hazard spatial layer

Sp: is the population spatial layer

The number of people exposed to a flood is not the only aspect of interest when calculating flood exposure. We were also interested in assessing the number of infrastructures at risk of flooding. To create a vector layer that contains exposed infrastructures at a specific location, the spatial queries

allowed us to extract features in infrastructures map layer by their relation (intersection) with the flood hazard layer, using extract by location operation. Thus, flood risk related to infrastructures was defined as:

$$R_f = F_h \cap I_S \quad (2)$$

Were,

R_f: is flood risk for each territory

F_h: is the flood hazard spatial layer

I_S: is infrastructures spatial layer

Exposure by country was quantified as the ratio of population or infrastructures exposed to 100-year-flood compared to the total population or infrastructures of the basin. While exposure by return period was quantified as the ratio of total population or infrastructures exposed to related return period compare to total population or infrastructures of the basin. Then, exposure at the basin level was the ratio of population or infrastructures of the basin exposed to 100-year flood compare to the total population or infrastructures of the basin. Total element (population and infrastructures) of the basin were the sum of population pixels or infrastructures located in the Congo basin.

4.3.2. Risk hotspots assessment

The first step in the flood hotspots analysis for the Congo River Basin was to examine flood hazard in terms of available spatial data on flood occurrence. The desirable analysis would be the probabilities of occurrence of a flood hazard in a specific time period. Unfortunately, detailed probabilistic analysis of this type does not exist for flood hazards in the Congo River Basin. Even without detailed analysis, however, it is still possible to distinguish between areas of higher and lower risk using flood occurrence data (UNISDR, 2005). Occurrence of flood and location can be imaged by satellite or captured through modelling. In addition, risk hotspots can also be determined using the exposure of people to flood.

Data sets on historical flood occurrence have been explored, and integrated in the analysis. Over time, Dartmouth Flood Observatory (DFO), actually Colorado Flood Observatory (https://floodobservatory.colorado.edu/) (Brakenridge, 2020) has compiled a list of extreme flood events from diverse sources and georeferenced to the nearest degree from 1985 to date (Brakenridge, 2020). This data provides spatial information on flood occurrence against which flood areas from the model were evaluated. The LISFLOOD-FP model output (Sampson et al., 2015) such as the flood hazard map for different return periods (5, 20, 50, 75 and 100-year) were used to identify flood hotspots for the Congo River Basin. To characterize 100-year flood exposure hotspot, the exposed population of the 374 territories were weighted and the resulting index (0–1) was used to classify each territory within the index class. The risk was classified according to the

index class and the map has been generated based on the number of territory per class. The weighted index for each territory is calculated as:

$$W_T = \left(\left(\frac{\% P_i}{\% P}\right)\left(\frac{P_i}{P}\right)\right) \times 1000 \quad (3)$$

Were,

W_T: is weighted index for each territory,

$\% P_i$: is percentage of exposed population per territory,

$\% P$: percentage of total population of 374 territories

P_i: is number of population per territory,

P: Total population of 374 territories.

4.3.3. Evaluation process

The developed global maps were tested in different locations in CRB, in order to evaluate the capability of the produced flood maps in detecting flood areas. Several sources including the Dartmouth Flood Observatory and NASA's 250 m resolutions Near Real Time Flood Map (NRTFM) (NASA, 2020) were used. The 2019-2020 flood imagery was taken from the NASA's Near Real Time Flood Map. The NASA NRTFM uses Moderate Resolution Image Spectroradiometer (MODIS) imagery to capture flood events globally, and stores them online in an open-access domain. Using over two weeks of data ensured that the entire event (maximum extent) was captured. The NASA's flood imagery was compared with the LISFLOOD-FP's flood extend output of 50-year return period. The 2019-2020 floods were one of the most devastating floods in the basin and are comparable to the 1960s flood in term of extend and impact (Reliefweb, 2019). These flood events had probably an estimated return period of around 50 years (Thinkhazard, 2020). The 50-year return period was reported with no indication of how the value was estimated. In this evaluation, the mentioned return period, both reported and modelled, do have their associated uncertainties that needs to be considered. In order to preserve the detail of the model resolution (~90 m), and because comparison needs to be carried out at the same spatial resolution, the MODIS imagery outputs were resampled to ~90 m resolution using the nearest neighbour method. The modelled extent maps for a 50-year flood was than compared against reported flood extents from NASA's Near Real Time Flood Map Products. LISFLOOD-FP flood extents and the observed NASA extents overlap was evaluated in terms of the number of pixels that showed agreement, overprediction, and underprediction. The performance score was chosen to evaluate model performance (model fit, and the proportion of flood captured). Critical success index (CSI) score or the $F^{<2>}$ is a comprehensive performance scores (Stephens et al., 2014) and estimated as:

$$CSI = \frac{F_m \cap F_0}{F_m \cup F_0} \quad (4)$$

Were,

$F_m \cap F_0$: is the intersection of the modelled and observed flood extent,

$F_m \cup F_0$: is the union of modelled and observed extent.

The CSI ranges from worst (0) to best (1). The CSI has been shown to favourably bias larger floods (Wing et al., 2017). However, because the floods compared in this study have a similar return period, CSI was assumed appropriate. The CSI was applied to the LISFLOOD-FP flood maps and NASA's GSFC MODIS Flood Mapping Products. Such evaluation allows us to investigate the performance of the flood hazard maps in identifying flood extent where official flood maps do not exist. The performance metric used in the analysis of the flood models is commonly used in flood model assessments and for forecast verification (Dorotti et al., 2016; Sampson et al., 2015; Bernhofen et al., 2018; Wings et al., 2017; Trigg et al., 2017; Jannis & Trigg, 2019). Visual observation allowed us to compare the flood-prone areas identified by the DFO data were consistent with that produced by the model.

5. RESULTS

5.1. Hazard assessment

The flood hazard maps proved to be consistent with known and reported flood areas. The map (Fig.9) indicates geographic location of NASA's floods (Modis imagery) and flood events during 1985 – 2010, reported by the public global database, the Dartmouth Flood Observatory. According to the Dartmouth Flood Observatory (DFO), there are 34 territories in the CRB reported as having experienced large flooding events that have confirmed our results. Besides, this study revealed 374 territories throughout the CRB predicted as being at risk of fluvial flooding. The biggest difference between modelled and observed events occurs in the centre, South and North of the CRB. This is likely at least partly due to the optical sensor (MODIS) used by Dartmouth Flood Observatory being obscured by clouds and its coarser resolution of 250 m. In addition, DFO data shows only floods that happened in the last 2 decades, rather than the potential to flood, as shown by the flood model. Not all areas at risk of flooding will have flooded and additionally, DFO data can have trouble detecting urban flooding and flooding under vegetations, both of which are simulated by the hazard data model. The regions with few reported flood impacts are the least populated areas of centre, North and South of the CRB.

The overlap of the observed and modelled extents and the performance scores are represented in Figure 10. The results indicate that there is an agreement in term of the location of flood for both

observed and modelled. However, differences persist in term of flood extents. Batanga, Lufira,Oubangui and Congo stand out as the areas in which the models perform well. The CSI scores which are acceptable (> 0.5) in these areas, are likely a reflection of the areas' narrow confined floodplain compared to Kwa, and Lualaba which showed poor value of CSI scores (< 0.5), may be due to large areas of floodplain with many bifurcations.

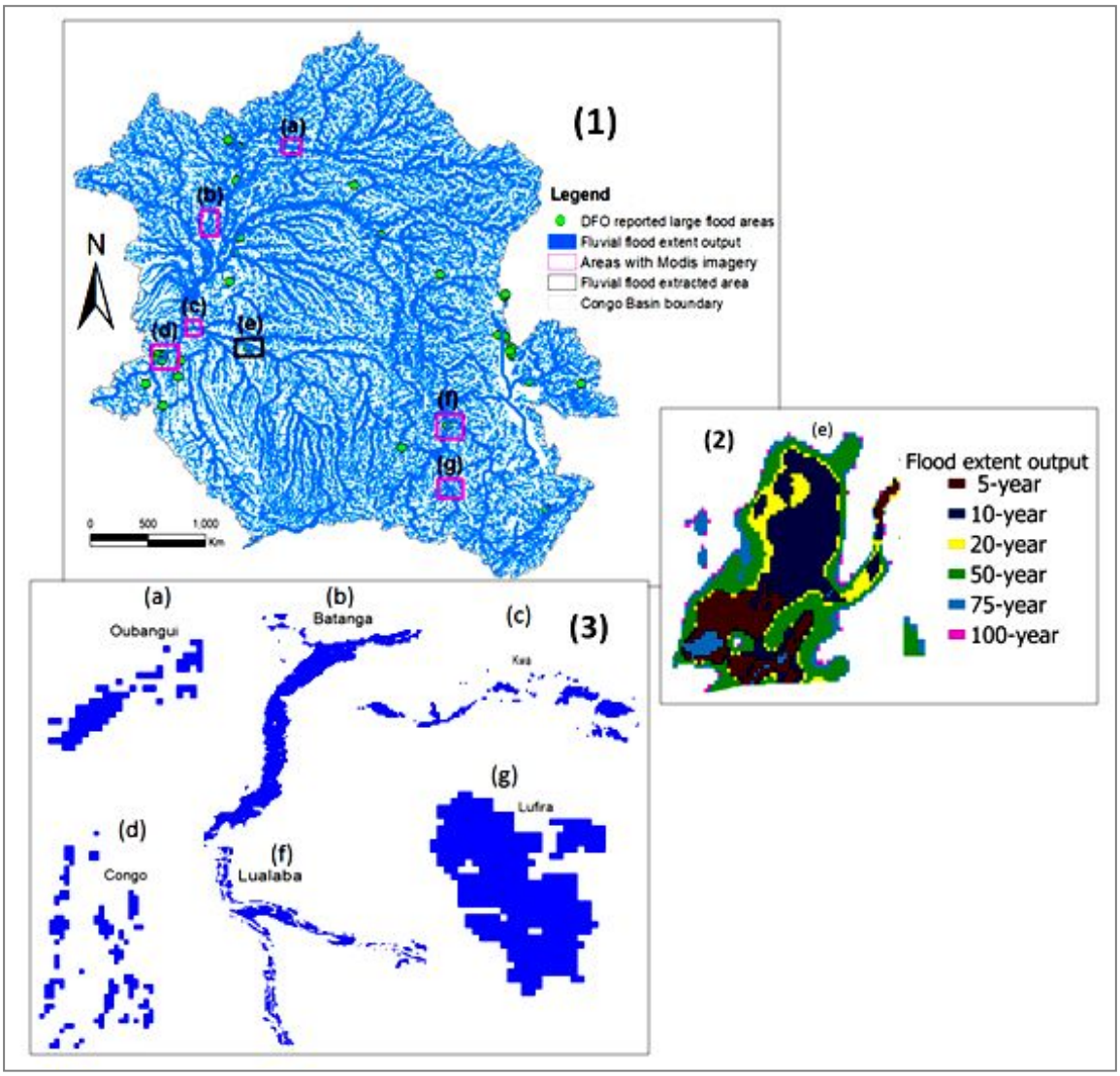

Figure 9: (1) Congo basin fluvial flood map for 5, 10, 20, 50, 75,100-year return period and location of reported flood from DFO. (2) Flood extent for different return period extracted from area (e). (3) MODIS imagery of 2019-2020 flooding for area (a,b,c,d,f,g).

For validation, the performance metrics used for flood forecast verification (CSI) shows different value of CSI scores (Fig.10). The CSI scores for different analysed areas in the basin is 0.51 for Oubangui, 0.64 for Batanga, 0.42 for Kasai, 0.60 for Congo, 0.71 for Lufira and 0.46 for Lualaba. The disagreement can be attributed to the flooded areas captured by NASA's satellite (good

temporal but limited spatial resolution) that are not connected to river within the modelling domain. These include lakes that are not connected to the floodplain and may be flooded perennially or seasonally by rainfall. Further, there are errors in the coarse representation of the flood areas.

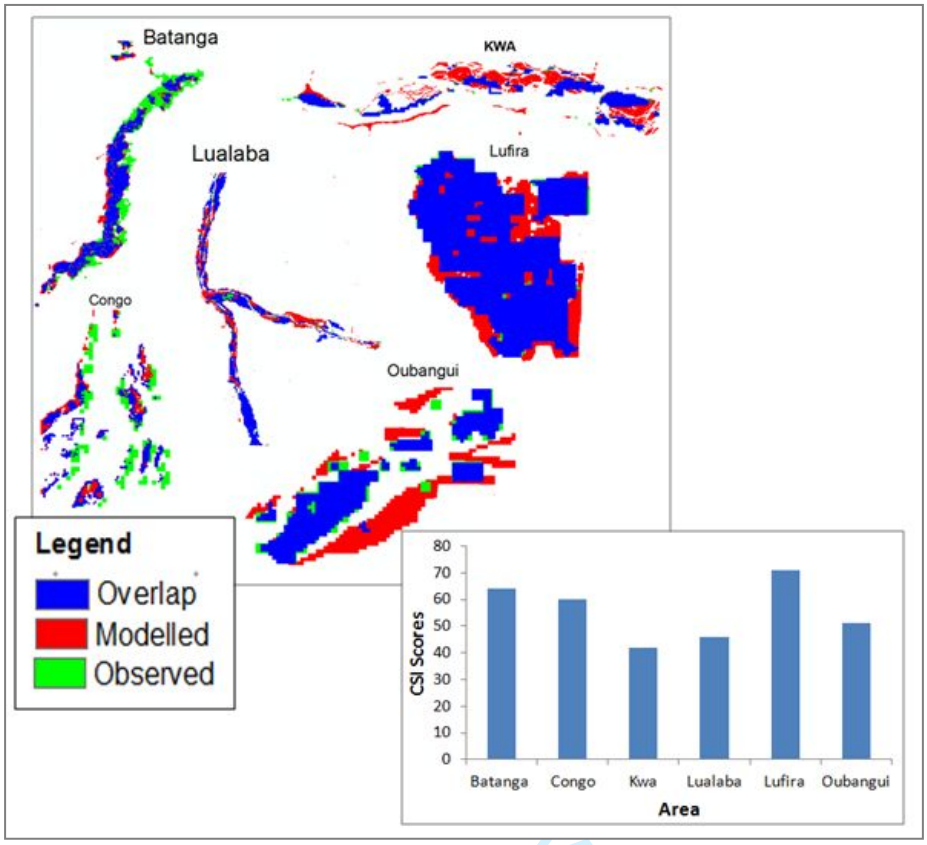

Figure 10: Overlap of individual model extent for return period flood of 50-years and MODIS observed flood extent for Oubangi, Batanga, Kwa, Congo, Lufira and Lualaba.

Not all areas at risk of flooding will have flooded and that NASA data can have trouble detecting urban flooding and flooding under vegetation, both of which are simulated by the hazard data.

5.2. Regional risk analysis and exposure to floods

For the entire region of the CRB, we estimate the total number of people and the share of the population who are exposed to floods at the territory level. In the results presented, we examine exposure for 5, 10, 20, 50, 75 and 100-year return period floods. We aggregate the results at country and the basin level. About 2.65% of present day population and 3.67% of infrastructure are exposed to flood (Table 2).

Table 2: Population and infrastructures exposed to flooding in the Congo River Basin

Exposed elements	Flood hazard						Exposure
	5-year	10-year	20-year	50-year	75-year	100-year	%
Population	571256	830995	1195406	1339714	1482381	2644124	2.65
Infrastructures	100	118	150	177	192	272	3.67

Flood risk analysis with respect to population revealed that approximately 0.57 % of the population is under 1 in 5 year flood hazard category, while 0.83 % and 1.2% are under 10 –year return period and 20-year return period flood category respectively. For 50-year return period flooding, 1.3 % of the CRB's population is already exposed. Exposure for the 75-year return period and 100-year return period flood events show that as hazard intensity increases, so does the exposure of population, 1. 49 % and 2.65 % respectively, (Table 3).

Table 3: Population exposed to flooding in the Congo River Basin

Countries	Flood hazard						Exposure
	5-year	10-year	20-year	50-year	75-year	100-year	%
Democratic Republic of the Congo	411918	622084	915751	1040413	1145619	1538497	1.54
Rwanda	30151	29261	24099	14313	12355	142797	0.14
Cameroun	2557	5407	6815	7873	8514	13843	0.01
Angola	1254	1673	2044	1576	1855	5076	0.01
Tanzania	14665	18057	17123	11254	12938	74006	0.07
Zambia	6749	8978	9783	7957	8583	34728	0.03
Burundi	30406	30621	25972	15064	17132	179142	0.18
Republic of the Congo	47980	65657	94032	115462	132737	155713	0.16
Central Africa Republic	25576	49257	99787	121144	147306	500323	0.50
Total	571256	830996	1195406	1335057	1487039	2644125	2.65
Exposure(%)	0.57	0.83	1.20	1.34	1.49	2.65	-

Following the analysis of the flood footprints on the infrastructure elements, a basin-wide aggregate of flood impact on infrastructure is presented. Fig. 11 shows the results for infrastructure exposed to all return period flooding and the results are reflective of the whole basin. Risk to infrastructure is extensive. The risk was greatest for places of worship where many churches are built in the floodplain. In the mega-city of Kinshasa for example, all places of worship situated at a distance of 50 m to the river are frequently flooded. Flood causes significant damage to fuel stations, schools and public buildings.

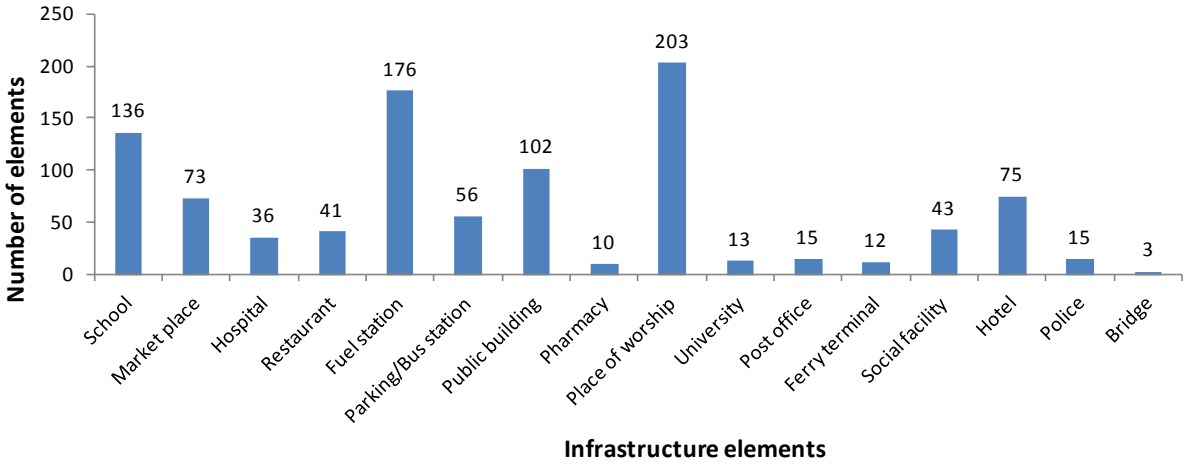

Figure 11: 100-year-return period flood and exposed infrastructure in the Congo Basin

Flood risk analysis with respect to infrastructure revealed that 1.35 % of assets are under the 5-year return period flood category, 1.59 % at 10 year, 2.01 % at 20-year, 2.39% at 50-year, 2.66% at 75- and 3.67% at 100-year return period (Table 4).

Table 4: Infrastructures exposed to flooding in the Congo River Basin.

Countries	Flood hazard						Exposure
	5-year	10-year	20-year	50-year	75-year	100-year	%
Democratic Republic of the Congo	75	83	112	133	145	184	2.48
Rwanda	8	12	12	11	12	14	0.19
Cameroun	1	2	2	3	3	3	0.04
Angola	0	0	0	0	0	0	0.00
Tanzania	3	4	4	1	1	4	0.05
Zambia	1	3	3	3	4	4	0.05
Burundi	10	11	11	10	12	33	0.45
Republic of the Congo	0	0	1	7	10	16	0.22
Central Africa Republic	2	3	4	9	10	14	0.19
Total	100	118	149	177	197	272	3.67
Exposure(%)	1.35	1.59	2.01	2.39	2.66	3.67	-

Risk increases with the return period (Fig. 12), but there is a big change from 75 to 100-year exposure. The important value for the 100-year return period might be explained by the fact that the total flooded area doesn't follow the same pattern, or are there some significant populated areas that suddenly become inundated between 75 and 100 year.

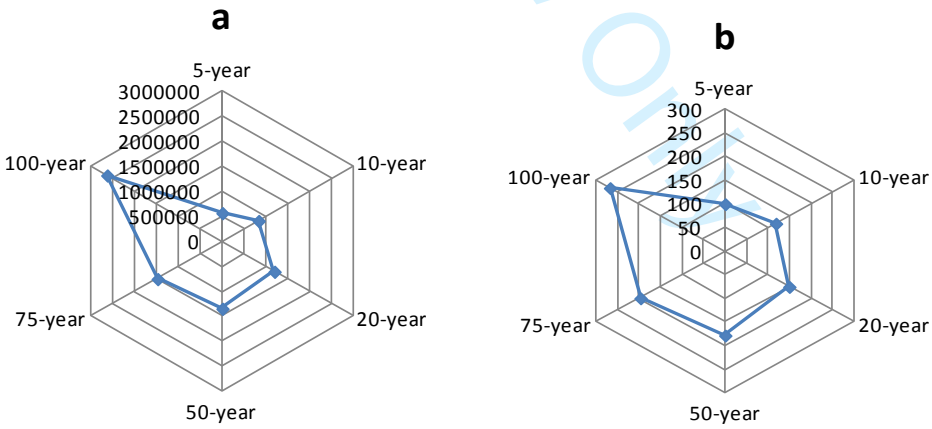

Figure 12: Spider diagram in case of: (a) exposed population, (b) exposed infrastructures

These regional results on exposure are not evenly distributed across countries. The spatial analysis also allows us to examine the distribution of exposed population with regard to all return period floods. Basin wide analysis identifies risk areas of high exposure along the Congo River main channel (Fig. 13). The aggregate results show a monotonic increased exposure with flood return period. Many zones of the CRB are exposed to floods which affect 374 of the Basin's 525

territories. Regions were affected differently according to their factor of risk. Lowland areas like the Cuvette Centrale were more exposed to floods, while mountainous areas like South East, North and South of the CRB were less exposed. One of the risk factors within the CRB might be the population density and its proximity to the river system, because of the importance of rivers for economic transportation (Trigg et al., 2020). In terms of absolute and relative risk of population and infrastructure, the DRC has the greatest exposure compared to other basin countries. This is primarily due to the proportion of DRC in the Congo Basin, 62% of the total basin area and 74% of the total basin population (Trigg et al., 2020). Overall, in the CRB the results show that there is a strong link between flood hazards and population settlement setting.

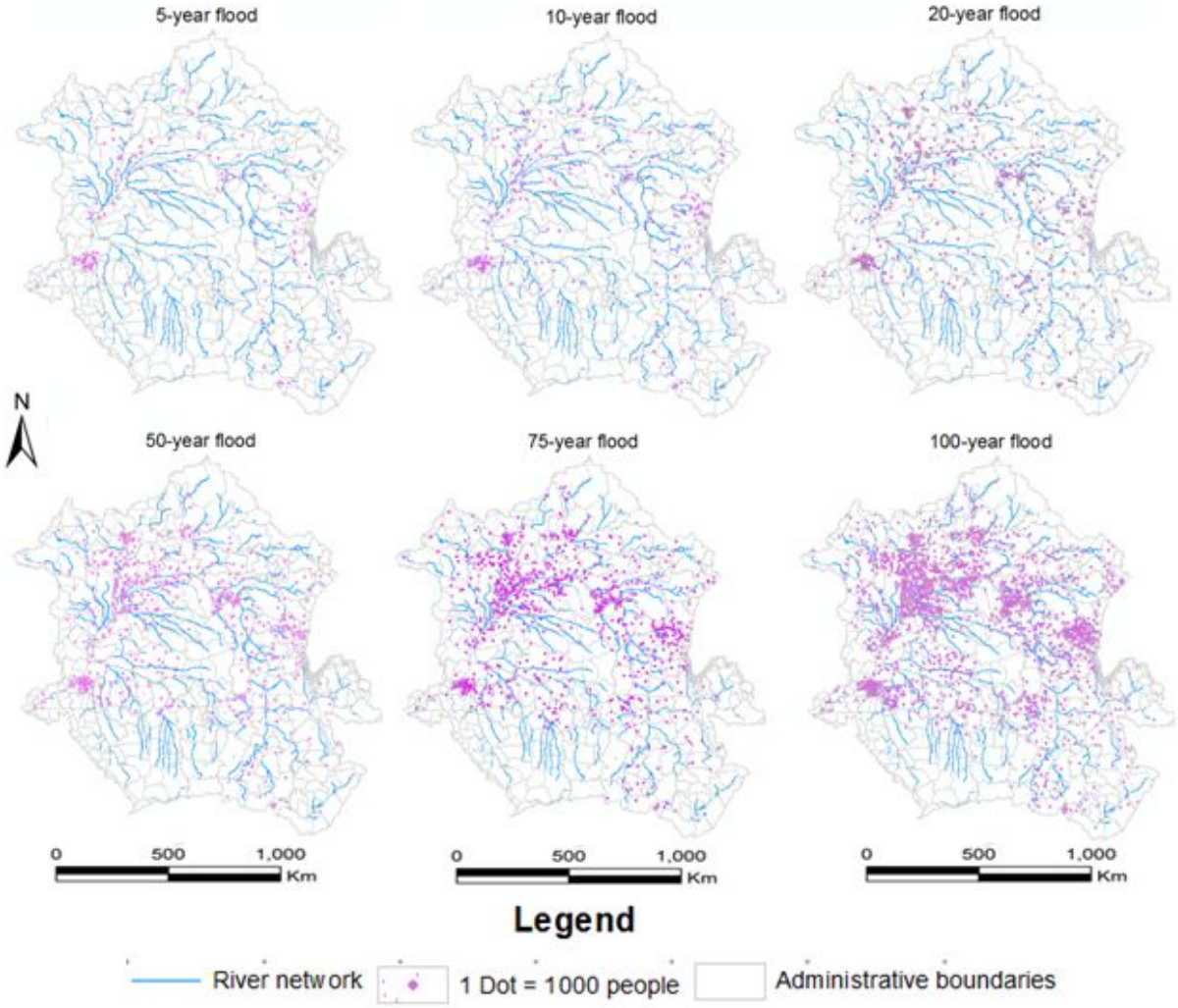

Figure 13: Dot density map showing exposed population in case of a: 5, 10, 20, 50, 75, and 100-year flood.

The territory level analysis (Fig. 14) shows that the most exposed territories represent 1% of total exposure which is estimated at 2.65% of the basin's population. Bomongo has a large relative exposure and Kinshasa has a large absolute exposure. These territories have high exposure likely

due to their low topography within the cuvette centrale and location along the navigable rivers. Low topography and location near the river are factors that increase flood risk during a flood event.

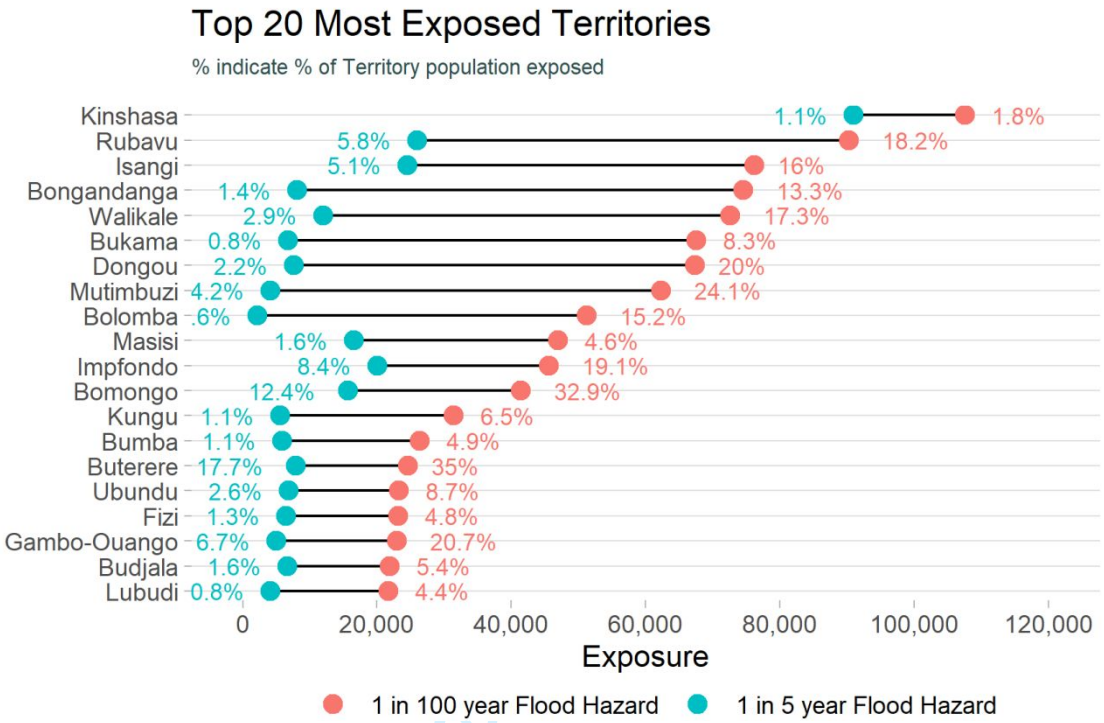

Figure 14: The 20 most exposed territories in the Congo River Basin

5.3. Risk hotspot assessment

Flooding risk hotspots maps were produced by considering areas in which high occurrence of flooding coincides with high exposure based on flood hazards and risk analysis. The output of the risk assessment and distribution of areas with different risk classes are shown in Figure 15. The risk pattern that emerged from this study indicates that 38 territories are flood hotspots risk areas due their high exposition in the Congo River Basin. Flood estimates for Congo River Basin show marked spatial variability. Flood hazard analysis brought out zones of high risk such as Kinshasa in the Southwest; Dongou and Bangui in the North; Bongandanga, Bolomba, Imfondo and Bomongo in the centre; Kisangani and Walikale in the Northeast. Vulnerability indicators (population, and basin topography) might be more important contributors to the degree of risk than the hazard in some cases. Considering risk as a function of hazard and vulnerability, five classes (Table 5) based on a weighted index of exposed population was established.

Table 5: Flood risk hotspots class

Weighted index class	Number of territories	Risk class
0.0-0.1	336	No risk hotspot
0.2-0.3	18	Low
0.4-0.5	8	Moderate
0.6-0.7	4	High
0.8-1	8	Very High

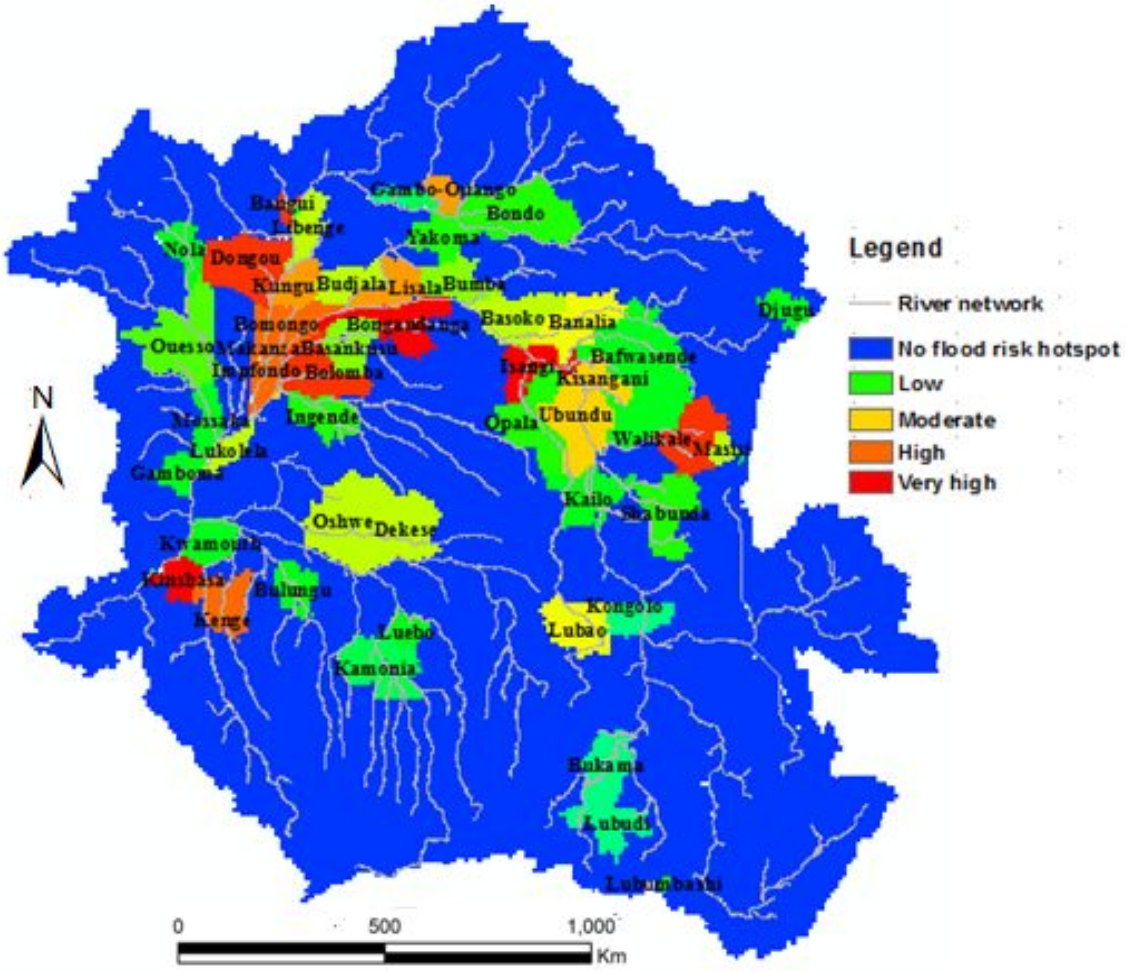

Figure 15: Hotspots for 100-year flood risk in the Congo River Basin

6. DISCUSSION

While fluvial flood risk for many developing countries is still unmapped, new global data has allowed an improved understanding of flood hazard and risk in the Congo Basin. Global flood models have therefore proved useful for flood risk analysis at regional scales (Bates, 2012; Trigg et al., 2016). The model showed a good agreement at Batanga, Lufira and Congo. This suggests that the models perform well at estimating the reported flood. The differences are apparent in the critical success index where the model showed an overprediction at three sites. This could be due to the

fact that detailed channel information at Kasai, Lualaba and Oubangui might not be well captured in the global model. Even if an improved connectivity offered by higher spatial resolution is evident in some sites, connectivity provided by small channels which has a significant effect on the hydraulics of floodplain might be absent in other sites (Bernhofen et al., 2018). Further, a better representation of bifurcation would improve the performance of both 1D and 2D sub-grid models in areas of high bifurcation, such as floodplains (Mateo et al., 2017). However, discrepancies between observed and global models indicate caution should be used in their application, particularly at fine scales (Bernhofen et al., 2018; Trigg et al., 2016). Nonetheless, their application in the Congo River Basin can be extremely helpful for predicting flood hazard and risk. Such studies can also increase the preparedness of populations and reduce catastrophic impacts (Dottori et al. 2016). Flooding risk in the CRB have been delineated by overlaying three datasets: the flood hazard map, the areal administrative units and a population dataset. The identified risk areas (based on exposed population and infrastructure) are distributed along the Congo River main channel, rivers confluences, and floodplains. These hydrological factors linked to settlement are often the most important factor in flood disasters and determine the vulnerability of an area. People have increasingly occupied floodplains areas for settlements and agricultural purposes, making themselves more vulnerable to flooding and increasing the risk (Hazarika et al., 2018). Considering significant impacts in low elevation floodplains, the Congo River main channel flooding due to its topography might be one of the causes of the higher risk.

Aggregate floods risk analysis results show that exposure monotonically increase with flood return period. But it has been observed from particular territories that some areas with less population were affected the most. Furthermore, the results illustrate a link between flood hazard and population settlement settings. Less populated zones are reported to be less affected. This study presents findings on flood risk in the Congo Basin, how it changes under different return periods, and whether exposure is unevenly distributed with flood areas identified mostly along the lowland of Congo River main channel. As regard to infrastructures, the aggregated analysis presented here shows that schools, fuel stations and places of worship are more prone to flooding than others. These exposures illustrate the socio-economic ambivalence between rural area and cities in term of socio-economic facilities. In fact, in the Congo Basin most of the infrastructure, such as schools, hospitals, fuel stations, hotels and public buildings are located in the main cities. Such uneven distribution and concentration of socio-economic facilities at cities increase flood risk and can exposes the basin to high economic loss during flood event. At a country level, Angola, Cameroon, Tanzania and Zambia are less exposed because their shares of basin area are rural and almost uninhabited. Conversely, the Democratic Republic of the Congo, Rwanda, Burundi, Republic of the

Congo and the Central Africa Republic are more exposed. All these countries have populated cities located along rivers where socio-economic facilities such as schools, hospitals, fuel stations, hotels are concentrated. For instance, Kinshasa in the Democratic Republic of the Congo and Brazzaville in the Republic of Congo are two mega cities located along the main Congo River, while Bangui in the Central Africa Republic and Buterere in Burundi are located on Oubangui river and lake Tanganyika respectively. Trigg et al. (2020) also confirm the uneven distribution of the population within the Congo Basin where low population density areas are away from navigation channels, while populated areas are located along rivers. Another observation is that in the southern and northern part of the basin, there are also populated cities along rivers which are not exposed to flood to the same extent as the central part. These differences demonstrate that follow-up actions, such as exposure dataset refinement should have a higher priority for flood risk analysis (Trigg et al., 2016).

With regard to relative exposure, most of the exposed territories are within the centre in the tropical humid region. This central part of the basin is known to be the Cuvette Centrale depression and has high exposure to flood even with less populated centers such as Bomongo, Impfondo, Dongou, Bongandanga, Bolomba Isangi and Maknaza. The high exposition of low populated area highlights the vulnerability of a particular location such as floodplain to being negatively affected by recurrent fluvial flood. Cuvette Centrale depression is characterise by massive floodplain of which settled people are prone to fluvial flood. However, certain practices for adapting to the risk of flooding, such as houses on stilts are put in place by the population. Hotspots analysis is intended to reveal areas of highest risk from flood hazards. The study illustrates both their damaging potential and the spatial distribution of risk. The hotspots map shows risk in the cuvette centrale, and the east of the basin. Centre and east hotspots are related to population living in the lowland area along main rivers. Conversely, in the west and the north of the Congo Basin, high risk is related to population density rather than location. The hotspots areas identify by the study follow the same pattern as of the DFO. This similarity reveals the fact that DFO detects only large floods and small or medium floods are generated by hydrodynamic models. There might be a distinct seasonality to risk posed by floods. Whereas the North zone has hotspots during the October-November rainy season, the Northeast zone is prone to floods during the December – April rainy season. In the Southwest and centre of the CRB, flood risk is during December-January rainy season. Thus, flood planning and preparedness is necessary not only on hotspots areas but also on “hotseasons”. The results demonstrate that exposure varies markedly in CRB, suggesting that population density and locations are the main factors of exposure. Moreover, exposure estimation undertaken in this study may substantially overestimate population at risk in some areas and underestimate them in other

areas. The use of gridded population data for risk is only indicative of exposed population. This previous viewpoint held that gridded population data is indicative because no method exists to validate the population data globally. However, researchers are currently challenging this view by demonstrating that Night-Time Light (NTL) captures population better than prior work which relied on algorithm or building identification to generate local estimates of population (Mellander et al. 2015). In addition, population estimates originate from census data obtained at only a coarse administrative unit. Thus, population data should be used with some caution at a fine scale. It is why Smith et al. (2019) state that when these data are intersected with the hazard data, the majority of the modelled hazard area does not generate exposure (Smith et al., 2019).

7. Conclusion

This study has shown the great potential of identifying exposure to flooding in the CRB region using global data. The intention of this study was to explore the use of different global data sources for predicting and estimating flood risk. The key point is the performance of global data in identifying flood areas in the CRB. We found that a combination of flood hazard maps with different layers can perform this task with reasonable accuracy. We have demonstrated that global data can make up for the absence of ground data for the purpose of flood risk assessment in developing countries. We highlight that the limitations arising from the use of limited accuracy population and infrastructure data may not be significant when we are interested in the identification of flood risk at a regional scale, but can be quite critical for flood risk analysis at the small scale. Throughout 525 territories, 374 are exposed to different flood periods and 10 % of these territories are categorised as hotspots of flood risk. Flood risk pattern identified by the study could be further analysed, and steps could be taken by researchers to confirm flood seasonality and pattern within the basin. Exposure distribution reflects the characteristic features of the region, which, in turn, influences the hazard, vulnerability and the risk from flooding. Settlement location and terrain topography seem to worsen flood risk for population in the basin. This study suggests that flood risk derived from global data may lead to flood hazard management challenges at national and regional scales of analysis and decision making, given the financial resource constraints for follow on small scale assessments. Identification of the most exposed areas can inform disaster prevention measures, including prioritization of intervention, for more detailed and localized risk assessments and emergency response strategies. Flood risk mapping could be used by policy makers and agencies in formulating flood mitigation policies and resource allocation, of which the main focus would be a decrease of the vulnerability and risk in flood hazard zones and the development of long-term land-use plans and multi-hazard risk management strategies.

Focusing on flood risk management rather than disaster relief would greatly benefit Congo Basin countries, cut costs for donors, and free up resources for promoting positive development that impact population livelihood. Through these analyses, international donors can focus attention and resources on high-risk regions. National authorities can use similar techniques to formulate proactive and effective risk management. This study exhibits the first and most important stage in developing flood responses by determining the flood hazards areas and the population that would be affected. Heavily affected areas have been identified and the flood exposure of the basin closely examined. In addition to the need for accurate flood risk reduction measures, considerable effort needs to be focused on basin scale response. It is now recognized that hydro-meteorological disasters such as floods are an integral component of hydrological system, and not just a matter of planning for emergency and humanitarian assistance at individual or family preparedness. This integrated approach links the upstream–downstream continuum but also improves the long-term environmental and social sustainability and poverty alleviation.

Acknowledgements

We thank the Royal Society-DFID for their financial support. This study was part of the CRuHM project under Africa Capacity Building Initiative (grants AQ150005 and FLR\R1\192057).

References

Alcántara-Ayala, I. (2002). Geomorphology, Natural Hazards, Vulnerability and Prevention of Natural Disasters in Developing Countries. Geomorphology 47, 107–124. https://doi.org/10.1016/S0169-555X(02)00083-1

Alsdorf, D., Beighley, E., Laraque, A., Lee, H., Tshimanga, R., O'Loughlin, F., Mahé, G., Dinga, B., Moukandi, G., & Spencer, R.G.M. (2016). Opportunities for hydrologic research in the Congo Basin. Reviews of Geophysics 54, 378–409. https://doi.org/10.1002/2016RG000517

Armenakis, C., Du, E.X., Natesan, S., Persad, R.A., & Zhang, Y. (2017). Flood Risk Assessment in Urban Areas Based on Spatial Analytics and Social Factors. Geosciences 7, 123. https://doi.org/10.3390/geosciences7040123

Baldassarre, G.D., Montanari, A., Lins, H., Koutsoyiannis, D., Brandimarte, L., & Blöschl, G. (2010). Flood fatalities in Africa: From diagnosis to mitigation. Geophysical Research Letters 37. https://doi.org/10.1029/2010GL045467

Barredo, J.I., Lavalle, C., & Ad De Roo. (2005). European flood risk mapping; EC DG JRC – Weather Driven Natural Hazards, Joint Research Center (Technical Report 32-800, pp. 251–260) European Commission

Bates, P.D., Horritt, M.S., & Fewtrell, T.J. (2010). A simple inertial formulation of the shallow water equations for efficient two-dimensional flood inundation modelling. Journal of Hydrology 387, 33–45. https://doi.org/10.1016/j.jhydrol.2010.03.027

Bates, P.D. (2012). Integrating remote sensing data with flood inundation models: how far have we got? Hydrological Processes 26, 2515–2521. https://doi.org/10.1002/hyp.9374

Bernhofen, M.V., Whyman, C., Trigg, M.A., Sleigh, P.A., Smith, A.M., Sampson, C.C., Yamazaki, D., Ward, P.J., Rudari, R., Pappenberger, F., Dottori, F., Salamon, P., & Winsemius, H.C.(2018). A first collective validation of global fluvial flood models for major floods in Nigeria and Mozambique. Environ. Res. Lett. 13, 104007. https://doi.org/10.1088/1748-9326/aae014

Bizimana, J., & Schilling, M. (2010). Geo-Information Technology for Infrastructural Flood Risk Analysis in Unplanned Settlements: A Case Study of Informal Settlement Flood Risk in the Nyabugogo Flood Plain, Kigali City, Rwanda. pp. 99–124. https://doi.org/10.1007/978-90-481-2238-7_6

Brakenridge, G.R. (2020). "Global Active Archive of Large Flood Events", Dartmouth Flood Observatory, University of Colorado, http://floodobservatory.colorado.edu/Archives/index.html (Accessed: 9th March 2020)

Bright, E. A., Rose, A. N., Urban, M. L., & Landscan. (2015). High-Resolution Global Population Data Set. TN, USA: Oak Ridge National Laboratory.

Bronstert, A. (2003). Floods and Climate Change: Interactions and Impacts. Risk Analysis 23, 545–557. https://doi.org/10.1111/1539-6924.00335

Christensen, J.H., & Christensen, O.B. (2003). Severe summertime flooding in Europe. Nature 421, 805–806. https://doi.org/10.1038/421805a

Center For International Earth Science Information Network-CIESIN-Columbia University. (2018). Centro Internacional De Agricultura Tropical-CIAT. Gridded Population of the World,Version3(GPWv3):PopulationDensityGrid.(2005).https://doi.org/10.7927/H4XK8CG

de Moel, H., Jongman, B., Kreibich, H., Merz, B., Penning-Rowsell, E., & Ward, P.J. (2015). Flood risk assessments at different spatial scales. Mitig Adapt Strateg Glob Change 20, 865–890. https://doi.org/10.1007/s11027-015-9654-z

Dilley, M., Chen, R.S., Deichmann, U., Lerner-Lam, A.L., Arnold M., Agwe, J., Buys, P., Kjekstad, Od., Lyon, B., & Yetman, G. (2005). Natural Disaster Hotspots: A Global Risk Analysis (World Bank Publication No. 05-34423). Washington,D.C.: The World Bank Hazard Management Unit.

De Sherbinin, A., & Adamo,s. (2015). Experience in mapping population and Poverty, Center for International Earth Science Information Network(CIESIN), Earth Institue, Columbia University. Retreive from https://www.un.org/en/development/desa/population/events/pdf/expert/23/Presentations/EGM-S6-deSherbinin%20Adamo%20presentation.pdf. (Accessed: 11th June 2020).

Dottori, F., Figueiredo, R., Martina, M.L.V., Molinari, D., & Scorzini, A.R. (2016). INSYDE: a synthetic, probabilistic flood damage model based on explicit cost analysis. Natural Hazards and Earth System Sciences 16, 2577–2591. https://doi.org/10.5194/nhess-16-2577-2016

Egbinola, C.N., Olaniran, H.D., & Amanambu, A.C. (2017). Flood management in cities of developing countries: the example of Ibadan, Nigeria. Journal of Flood Risk Management 10, 546–554. https://doi.org/10.1111/jfr3.12157

Eleutério, J. (2012). Flood risk analysis : impact of uncertainty in hazard modelling and vulnerability assessments on damage estimations (Doctoral dissertation).Retrieved from https://tel.archives-ouvertes.fr/tel-00821011/document. University of Strasbourg(Accessed: 22nd March 2020)

Eleutério, J., Hattemer, C., & Rozan, A. (2013). A systemic method for evaluating the potential impacts of floods on network infrastructures. Natural Hazards and Earth System Sciences 13, 983–998. https://doi.org/10.5194/nhess-13-983-2013

Eleutério, J., Martinez, D., & Rozan, A.(2010). Developing a GIS tool to assess potential damage of future floods. WIT Transactions on Information and Communication Technologies 43. https://doi.org/10.2495/RISK100331

EM-DAT, 2019. The international Desaster Database, Center for Research on the Epidemiology of Disaster. Retreive from https://www.emdat.be , acced: 22th August 2020.

Facebook Connectivity Lab & Center for International Earth Science Information Network - CIESIN. (2018). Retrieved from:http://ciesin.columbia. edu/data/hrsl/. USA: Columbia University (Accessed: 22nd April 2020).

Fortin Jean, P., Turcotte, R., Massicotte S., Moussa, R., Fitzback, J., & Villeneuve Jean-Pierre (2001). Distributed Watershed Model Compatible with Remote Sensing and GIS Data. I: Description of Model. Journal of Hydrologic Engineering 6, 91–99. https://doi.org/10.1061/(ASCE)1084-0699(2001)6:2(91)

Haensler, A., Jacob, D., Kabat, P., & Ludwig, F. (2013). Climate Change Scenarios for the Congo Basin (Climate Service Centre report No. 11, pp. 2192-4058). Hamburg, Germany.

Hazarika, N., Barman, D., Das, A.K., Sarma, A.K., & Borah, S.B. (2018). Assessing and mapping flood hazard, vulnerability and risk in the Upper Brahmaputra River valley using stakeholders' knowledge and multicriteria evaluation (MCE). Journal of Flood Risk Management 11, S700–S716. https://doi.org/10.1111/jfr3.12237

Hirabayashi, Y., Mahendran, R., Koirala, S., Konoshima, L., Yamazaki, D., Watanabe, S., Kim, H., & Kanae, S. (2013). Global flood risk under climate change. Nature Climate Change 3, 816–821. https://doi.org/10.1038/nclimate1911

Humanitarian Data Exchange (HDX)/UN Office for the Coordination of Humanitarian Affairs (OCHA). (2019). Retrieved from:https://data.humdata.org/. Washington,D.C.: United Nations Office for the Coordination of Humanitarian Affairs (Accessed: 22nd December 2019).

Change, I. P. on C., Protection, U. N. E., III, I. P. on C. C. W. G., Working, I. P. O. C. C., Science, I. P. on C. C. W. G., & Organization, W. M. (2001). Climate Change 2001: Synthesis Report: Third Assessment Report of the Intergovernmental Panel on Climate Change. Cambridge University Press.

IPCC (2012) Managing the Risks of Extreme Events and Disasters to Advance Climate Change Adaptation(n.d.). European Environment Agency. Retrieved from https://www.eea.europa.eu/data-and maps/indicators/direct-losses-from-weather-disasters-1/ipcc-2012-managing-the-risks (Accessd: 7th May 2020)

Jongman, B., Ward, P., & Jeroen, C. (2012). Global exposure to river and coastal flooding: Long term trends and changes. Global Environmental Change 22, 823–835. https://doi.org/10.1016/j.gloenvcha.2012.07.004

Jonkman, S. N. (2005). Global Perspectives on Loss of Human Life Caused by Floods. Natural Hazards, 34, 151–175. https://doi.org/10.1007/s11069-004-8891-3

Kundzewicz, Z. W., Kanae, S., Seneviratne, S. I., Handmer, J., Nicholls, N., Peduzzi, P., Mechler, R., Bouwer, L. M., Arnell, N. W., Mach, K., Muir-Wood, R., Brakenridge, G. R., Kron, W., Benito, G., Honda, Y., Takahashi, K., & Sherstyukov, B. (2014). Flood risk and climate change: Global and regional perspectives. Hydrological Sciences Journal, 59(1), 1–28. http://pure.iiasa.ac.at/id/eprint/10982/

Lim, J., & Lee, K. (2018). Flood Mapping Using Multi-Source Remotely Sensed Data and Logistic Regression in the Heterogeneous Mountainous Regions in North Korea. Remote Sensing 10, 1036. https://doi.org/10.3390/rs10071036

Mason, D.C.; Schumann, G.; Bates, P. (2011).Data utilization in flood inundation modelling. Flood Risk Sci. Manag.

Mateo, C. M. R., Yamazaki, D., Kim, H., Champathong, A., Vaze, J., & Oki, T. (2017). Impacts of spatial resolution and representation offlow connectivity on large-scale simulation offloodsHydrol. Earth Syst. Sci.215143–63 [49]

Merz, B., Aerts, J., Arnbjerg-Nielsen, K., Baldi, M., Becker, A., Bichet, A., Blöschl, G., Bouwer, L. M., Brauer, A., Cioffi, F., Delgado, J. M., Gocht, M., Guzzetti, F., Harrigan, S., Hirschboeck, K., Kilsby, C., Kron, W., Kwon, H.-H., Lall, U., & Nied, M. (2015). Floods and climate: Emerging perspectives for flood risk assessment and management. Natural Hazards and Earth System Sciences, 14(7), 1921–1942. https://doi.org/10.5194/nhess-14-1921-2014

Messner, F., & Meyer, V. (2006). Flood damage, vulnerability and risk perception–challenges for flood damage research, in: Flood Risk Management: Hazards, Vulnerability and Mitigation Measures. pp. 149–167. https://doi.org/10.1007/978-1-4020-4598-1_13

Milly, P.C.D., Wetherald, R.T., Dunne, K.A., & Delworth, T.L. (2002). Increasing risk of great floods in a changing climate. Nature 415, 514–517. https://doi.org/10.1038/415514a

Munich Re., 2014. NatCatSERVICE Database (Munich Reinsurance Company). Retrieved from https://www.munichre.com/topics-online/en/climate-change-and-natural-disasters.html. Germany: Munich (Accessed: 15th April2020)

NASA, (2020). National Aeronautics and Space Administration, Near Real-Time Flood Mapping. Retrieve on https://floodmap.modaps.eosdis.nasa.gov/getTile.php?location=010E000S&day=15&year=2020&product=14 (accessed, 22th July 20202)

NSO, (2016) National Statistical Office OF Burundi: Household Socio-Economic Characterisctics, retrieve on : http://www.nsomalawi.mw/images/stories/data_on_line/economics/ihs/IHS3/IHS3_Report.pdf. (accessed on 22th, May 20120)

Neal, J., Schumann, G., & Bates, P. (2012a). A subgrid channel model for simulating river hydraulics and floodplain inundation over large and data sparse areas. Water Resources Research 48. https://doi.org/10.1029/2012WR012514

Neal, J.C., Bates, P.D., & Schumann, G. (2012b). A simple model for simulating river hydraulics and floodplain inundation over large and data sparse areas. Paper presented at AGU Fall Meeting Abstracts 34, EP34A-05.

Peduzzi, P., Dao, H., Herold, C., & Mouton, F. (2009). Assessing global exposure and vulnerability towards natural hazards: the Disaster Risk Index. Natural Hazards and Earth System Sciences 9, 1149–1159. https://doi.org/10.5194/nhess-9-1149-2009

Pokam, W. M., Bain, C. L., Chadwick, R. S., Graham, R., Sonwa, D. J., & Kamga, F. M. (2014). Identification of processes driving low-level westerlies in west equatorial Africa, J. Clim., 27(11), 4245–4262.

Roo, A., De, A., Wesseling, C.G., Deursen & Deursen, W.P.A. (2000). Physically based river basin modelling within a GIS: the LISFLOOD model. Hydrological Processes 14, 1981. https://doi.org/10.1002/1099-1085(20000815/30)14:11/123.3.CO;2-6

Reliefweb, Office for the Coordination of Humanitarian Affairs (OCHA) 2020. Retrieved from: https://reliefweb.int/disaster/fl-2019-000160-cog. Washington,D.C.: United Nations Office for the Coordination of Humanitarian Affairs (Accessed: 22nd April 2020).

Safaripour, M., Monavari, S., Zare, M., Abedi, Z., & Gharagozlou, A. (2012). Flood Risk Assessment Using GIS (Case Study: Golestan Province, Iran). Polish Journal of Environmental Studies 21, 1817–1824.

Samarasinghe, S.M.J.S., Nandalal, H., Weliwitiya, D.P., Fowze, J. s, Hazarika, M., & Samarakoon, L. (2010). Application of remote sensing and gis for flood risk analysis: A case study at Kalu-Ganga River, Sri Lanka. International Archives of the Photogrammetry, Remote Sensing and Spatial Information Sciences - ISPRS Archives 38, 110–115.

Sampson, C.C., Smith, A.M., Bates, P.D., Neal, J.C., Alfieri, L., & Freer, J.E. (2015). A high-resolution global flood hazard model. Water Resour Res 51, 7358–7381. https://doi.org/10.1002/2015WR016954

Schumann, A. (2011). Flood risk assessment and management: How to specify hydrological loads, their consequences and uncertainties. https://doi.org/10.1007/978-90-481-9917-4

Schumann, G.J.-P., Neal, J.C., Voisin, N., Andreadis, K.M., Pappenberger, F., Phanthuwongpakdee, N., Hall, A.C., & Bates, P.D. (2013). A first large-scale flood inundation forecasting model. Water Resources Research 49, 6248–6257. https://doi.org/10.1002/wrcr.20521

Shivaprasad, S. V., Parth, S.R., Chakravarthi, V., & Srinivasa, R.G. (2018). Flood risk assessment using multi-criteria analysis: a case study from Kopili River Basin, Assam, India. Geomatics, Natural Hazards and Risk 9, 79–93. https://doi.org/10.1080/19475705.2017.1408705

Schumann, G.; Bates, P.D.; Horritt, M.S.; Matgen, P.; & Pappenberger, F. (2009). Progress in integration of remote sensing- derived flood extent and stage data and hydraulic models. Rev. Geophys. 2009, 47.

Schumann, G.J.P., Brakenridge, G.R., Kettner, A.J., Kashif, R., & Niebuhr, E. (2018). Assisting Flood Disaster Response with Earth Observation Data and Products: A Critical Assessment. Remote Sensing 10, 1230. https://doi.org/10.3390/rs10081230

Smith, A., Bates, P.D., Wing, O., Sampson, C., Quinn, N., & Neal, J. (2019). New estimates of flood exposure in developing countries using high-resolution population data. Nature Communications 10, 1–7. https://doi.org/10.1038/s41467-019-09282-y

Smith, A., Sampson, C., & Bates, P. (2015). Regional flood frequency analysis at the global scale. Water Resources Research 51, 539–553. https://doi.org/10.1002/2014WR015814

Stephens, E., Schumann, G., & Bates, P. (2014). Problems with binary pattern measures for flood model evaluation Hydrol. Process. 28 4928–37

Trigg, M.A., Birch, C.E., Neal, J.C., Bates, P.D., Smith, A., Sampson, C.C., Yamazaki, D., Hirabayashi, Y., Pappenberger, F., Dutra, E., Ward, P.J., Winsemius, H.C., Salamon, P., Dottori, F., Rudari, R., Kappes, M.S., Simpson, A.L., Hadzilacos, G., & Fewtrell, T.J. (2016). The credibility challenge for global fluvial flood risk analysis. Environ. Res. Lett. 11, 094014. https://doi.org/10.1088/1748-9326/11/9/094014

Trigg, M.A., Birch, C.E., Neal, J.C., Bates, P.D., Smith, A., Sampson, C.C., Yamazaki, D., Hirabayashi, Y., Pappenberger, F., Dutra, E., Ward, P.J., Winsemius, H.C., Salamon, P., Dottori, F., Rudari, R., Kappes, M.S., Simpson, A.L., Hadzilacos, G., & Fewtrell, T.J. (2016). Aggregated fluvial flood hazard output for six Global Flood Models for the African Continent. University of Leeds (https://doi.org/10.5518/96)

Trigg M.A., Raphael M. Tshimanga, Preksides Ndomba, Felix A. Mtalo, Denis A. Hughes, Catherine A. Mushi, Gode B. Bola, Pierre M. Kabuya, Andrew B. Carr, Mark Bernhofen, Jeff Neal, Jules T. Baya, Felly K. Ngandu, & Paul Bates. (2020). Putting river users at the heart of hydraulics and morphology research in the Congo Basin. In Alsdorf, D., Bates, P.D., Tshimanga, R.M. (In review) Congo Basin Hydrology, Climate, and Biogeochemistry, Geophysical Monograph Series (In review) Washington, DC: American Geophysical Union

Tshimanga, R.M. (2012). Hydrological uncertainty analysis and scenario-based streamflow modelling for the Congo River Basin (Doctoral dissertation).Retrieved fromhttps://core.ac.uk/download/pdf/11984393.pdf, South Africa: Rhodes University repository (Accessed: 1st January 2020)

Tshimanga, R.M., & Hughes, D.A. (2014). Basin-scale performance of a semidistributed rainfall-runoff model for hydrological predictions and water resources assessment of large rivers: The Congo River, Water Resour. Res., 50,doi:10.1002/2013WR014310

Tshimanga, R.M., Tshitenge, J.M., Kabuya, P., Alsdorf, D., Mahe, G., Kibukusa, G., & Lukanda, V. (2016). Chapter 4 - A Regional Perceptive of Flood Forecasting and Disaster Management Systems for the Congo River Basin, in: Adams, T.E., Pagano, T.C. (Eds.), Flood Forecasting. Academic Press, Boston, pp. 87–124. https://doi.org/10.1016/B978-0-12-801884-2.00004-9

Tshimanga, R.M., Bola, G., Kabuya, P., Nkaba, L., Neal, J., Hawker, L., Trigg A.M., Bates,P., Hughes, A.D., Hughes, Laraque, A., Woods, R., & Wagener, T. (2020). Towards a framework of catchment classification for hydrologic predictions and water resources management in the ungauged basin of the Congo River: An a priori approach. In Alsdorf, D., Bates, P.D., Tshimanga, R.M. (Under preparation) Congo Basin Hydrology, Climate, and Biogeochemistry, Geophysical Monograph Series (In review) Washington, DC: American Geophysical Union

UN, International Strategy for Disaster Reduction. (2011). Global Assessment Report on Disaster Risk Reduction. Revealing Risk, Redefining Development. (Global Assessment Report). Retrievedfromhttps://sustainabledevelopment.un.org/index.php?page=view&type=400&nr=210&menu=35. Geneva: United Nations International Strategy for Disaster Reduction Secretariat (Accessed: 21st April 2020)

UN, International Strategy for Disaster Reduction. (2005). Natural disaster hotspots: a global risk analysis. (Global Assessment Report). Retrievedfromhttps://sustainabledevelopment.un.org/index.php?page=view&type=400&nr=210&menu=35. Geneva: United Nations International Strategy for Disaster Reduction Secretariat (Accessed: 21st April 2020)

UN, International Strategy for Disaster Reduction. (2015). Global Assessment Report on Disaster risk Reduction. Revealing Risk, Redefining Development. (Global Assessment Report). Retrieved from https://sustainabledevelopment.un.org/index.php?page=view&type=400&nr=210&menu=3. Geneva: United Nations International Strategy for Disaster Reduction Secretariat (Accessed: 2nd April 2020)

Ward, P.J., Jongman, B., Weiland, F.S., Bouwman, A., Beek, R. van, Bierkens, M.F.P., Ligtvoet, W., & Winsemius, H.C. (2013). Assessing flood risk at the global scale: model setup, results, and sensitivity. Environ. Res. Lett. 8, 044019. https://doi.org/10.1088/1748-9326/8/4/044019

Ward, P.J., Jongman, B., Salamon, P., Simpson, A., Bates, P., De Groeve, T., Muis, S., De Perez, E.C., Rudari, R., Trigg, M.A. & Winsemius, H.C. (2015). Usefulness and limitations of global flood risk models. Nature Climate Change, 5(8), pp.712-715

Wing, O., E J., Bates, P. D., Sampson, C. C., Smith, A., M., Johnson, K., A., & Erickson, T. A. (.2017) Validation of a 30 m resolution flood hazard model of the conterminous United States Water Resour. Res. 53 7968–86

Winsemius, H.C., Jongman, B., Veldkamp, T.I.E., Hallegatte, S., Bangalore, M., & Ward, P.J. (2015). Disaster risk, climate change, and poverty : assessing the global exposure of poor people to floods and droughts (No. WPS7480). The World Bank.

Yamazaki, D., Ikeshima, D., Sosa, J., Bates, P.D., Allen, G.H., & Pavelsky, T.M. (2019). MERIT Hydro: A High-Resolution Global Hydrography Map Based on Latest Topography Dataset. Water Resources Research 55, 5053–5073. https://doi.org/10.1029/2019WR024873

Yamazaki, D., Kanae, S., Kim, H., & Oki, T. (2011). A physically based description of floodplain inundation dynamics in a global river routing model. Water Resources Research, 47(4). https://doi.org/10.1029/2010WR009726